Nuclear Magnetic Resonance at High Temperature

JONATHAN F. STEBBINS

Department of Geology, Stanford University, Stanford, California 94305

Received February 20, 1991 (Revised Manuscript Received June 5, 1991)

Contents

I.	Introduction	1353
II.	Experimental Considerations	1354
III.	Applications to Organic Systems	1357
	A. Coal and Other Fossil Fuels	1357
	B. Pitch	1357
	C. Catalysis	1358
IV.	Silicates and Oxides	1358
	A. Crystalline Phases	1358
	B. Glasses and Liquids	1359
V.	Ionic Conductors	1360
	A. Crystalline Anionic Conductors	1361
	B. Crystalline Cationic Conductors	1362
	C. Amorphous Ionic Conductors	1363
VI.	Defects in Ionic Crystals	1363
VII.	Phase Transitions	1364
VIII.	Molten Salts	1365
IX.	The Transition from Molten Salt to Liquid Metal	1366
X.	Metals and Semimetals	1366
	A. Single Component Systems: Electronic Structure	1367
	B. Electronic Structure of Liquid Alloys	1367
	C. Electronic Structure of Solid Intermetallic and Intercalation Compounds	1367
	D. Atomic Structure and Dynamics in Liquid Metals	1368
	E. Defects and Trace Impurities in Solid Metals	1368
	F. Hydrogen in Solid Metals, Semimetals, and Hydrides	1369
XI.	Prospects for Future Work	1369

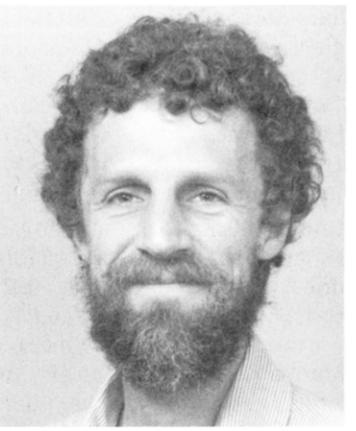

Jonathan Stebbins was born in Baltimore, MD in 1954, but has lived most of his life in the geologically more dramatic western United States. His combined interests in physical chemistry and the earth sciences first developed during his undergraduate work at Harvard. He obtained his Ph.D. in 1983 from the Department of Geology and Geophysics at the University of California, Berkeley, having worked primarily on the thermodynamic properties of silicate liquids. His interest in NMR spectroscopy developed through collaboration with researchers in the Berkeley chemistry department during a post-doctoral fellowship at the Lawrence Berkeley Laboratory. He has been on the faculty at Stanford since 1985. He and his research group are interested in the structure and dynamics of oxide and silicate liquids, glasses, and crystals, including both thermodynamic measurements and NMR studies at low and high temperature. They actively collaborate with several other groups in the Stanford School of Earth Sciences who are also studying the geochemistry of geological materials, including strong programs in surface structure and chemistry and in X-ray absorption spectroscopy.

I. Introduction

NMR spectroscopy has been used extensively to study materials at high temperature. Applications to specific systems such as ionic conductors, molten salts, and liquid metals have been reviewed relatively recently (as described in the appropriate sections below), but there do not seem to have been previous attempts to bring this literature together in one place. The subject is wide, and the questions posed diverse, but there are certainly common scientific themes as well as common experimental difficulties. For these reasons, and because of a number of very recent major advances, this review was undertaken.

"High temperature" means rather different things to different groups of scientists, of course: a physicist working on superconductors may use this term for 100 K, a biochemist for 50 °C, and a material scientist for 2000 °C. The literature search for this review revealed that an only slightly smaller range of usages can be found for "high temperature NMR". The bias of the author toward inorganic materials has lead the scope of this report to be restricted primarily to studies above 200 °C, with an attempt at completeness only for about the last 10 years. This temperature is also a natural dividing line because until very recently, most commercially available NMR probes were capable of reaching only about 150 °C to 250 °C, leading researchers to construct their own special equipment for higher temperature applications. The upper limit of NMR measurements has recently been extended to well above 2000 °C by a laser-heated system.[1] (The complications of making this division of subject matter are illustrated that the latter technology was in fact developed for commercialization by the Bruker Co.)

The motivations to carry out what may be technically rather difficult in situ high-temperature NMR studies vary. In many materials, of course, such as most molten salts, metals, and oxides, the liquid phase of interest cannot be quenched to room temperature. Even in glass formers, such as many silicates, the structure only at the glass transition temperature can be observed in a quenched sample. Crystalline solids often exhibit un-

0009-2665/91/0791-1353$09.50/0 © 1991 American Chemical Society

quenchable phase changes. And in any material, the energetics (and therefore the mechanisms) of dynamics can best be understood by exploring as wide a temperature range as possible.

Two broad classes of information have thus been sought in high-temperature NMR experiments. Structural information from NMR line shapes in solids has occasionally been obtained at elevated temperatures, and more applications will come with the improvement of high-temperature magic angle spinning (MAS) technology. A number of solid–solid phase transitions have been observed by this approach. More have been characterized by the effects of site symmetry changes on electric field gradient tensors. For the isotropically averaged narrow lines observed for liquids, the effects of atomic or molecular structure on chemical shift, and of electronic structure and dynamics on the Knight shift, have often provided important constraints on bonding and atom or ion association.

More commonly in high-temperature NMR studies, the unique range of time scales accessible by the technique (seconds to nanoseconds) has been exploited in dynamical studies. Studies of motional averaging of the wide lines common in solids can lead to quite specific and unambiguous results on rates and mechanisms of exchange among inequivalent sites, particularly when resolution is sufficient to clearly distinguish multiple peaks. Common in the literature of organic molecular liquids and solids, this approach has been applied at times to nonmolecular, inorganic phases as well. Single-crystal measurements, and, more recently, work at very high magnetic fields and with MAS, are particularly useful in studying site exchange in solids. In many systems (particularly those with high isotopic and chemical abundance of nuclei with high Larmor frequency), dipolar coupling to other nuclear spins or to unpaired electrons produces broad, featureless lines, whose motional narrowing is often the first feature observed as temperature is increased. In general, however, the relatively high activation energies for site exchange often mean that the transition from a static to a fully averaged line shape takes place over a rather narrow temperature interval, limiting the range over which dynamical information can be obtained. Recent high-temperature two-dimensional NMR studies have extended the dynamics sampled by line shape studies to much slower regimes (section IV.A).

Spin–lattice relaxation time measurements can often be made over much wider ranges of temperature than line-shape studies, and thus can be more useful than the latter to characterize changes in mechanisms of dynamics. Relaxation times in the rotating field reference frame ($T_{1\rho}$), and relaxation after site-selective excitation, can again extend the accessible time scale to relatively slow processes. However, relaxation-time data are generally more difficult to interpret, requiring assumption of a model for the relaxation mechanism and for the motion that causes it. The simple theory of Bloembergen, Purcell, and Pounds[2] (BPP) is often the starting point. The Arrhenius slope for T_1 (d ln T_1/d[$1/k_BT$]) is often used as an estimate of at least the apparent activation energy (E_A) for the relaxation process. If a T_1 minimum is observed, the equality of the inverse of the correlation time τ_c and the Larmor frequency at this point has often been used to estimate τ_c at at least one temperature, and to fix the "attempt frequency" (the preexponential term in an Arrhenian expression of the jump or exchange frequency, $\upsilon = \upsilon_0 \exp[-E_A/k_BT]$). The most thorough studies include measurements at more than one magnetic field to test the predictions from theory of frequency dependence, or use more than one isotope of a given element to vary either the resonance frequency or the quadrupolar or dipolar coupling terms. Many (most?) systems show divergence from BPP theory when data are complete enough, and a number of more general approaches have been taken that are described for specific materials. Some of these effects seem to be quite similar for superficially different systems (such as molten salts, ionic conducting solids, and liquid metals), suggesting the possibility of common underlying mechanisms.

The sensitivity of NMR to local dynamics means that insights into long-range transport such as diffusion, conductivity, and viscosity may be indirect, but can be taken advantage of to constrain specific atomic scale models of these processes. Direct measurements of diffusion by pulsed field gradient (PFG) techniques can be very useful, if diffusion rates are high enough and T_1 is not extremely short.

This review can only briefly introduce this wide range of different materials and processes. I have attempted, however, to show the common ground of the effects of atomic and molecular motion on NMR line shapes and relaxation times, and the relationships of these results with bulk properties of interest. Discussion will be primarily organized by type of material, progressing roughly from systems whose liquid phases are highly structured to those in which the liquids are relatively unstructured. However, we will first introduce some of the experimental dilemmas and solutions that are needed before these kinds of data can be obtained.

II. Experimental Considerations

A number of technical difficulties are inherent to NMR measurements at elevated temperatures. A good description of some of these considerations appears in a very recent review of experimental techniques for magnetic measurements in molten salts.[3] Some of the challenges of high-temperature NMR are shared with other high-temperature work and will not be discussed at length here, but a few comments may be useful.

For many materials, particularly reactive liquids, the superficially simple task of finding a suitable container often becomes a severe difficulty at high temperature. Because materials of substantial thickness located between samples and ratio frequency (rf) coils must be electrically insulating (or at least radio frequency transmitting), the use of metal or graphite sample containers is generally precluded. Solutions to problems of reaction between containers and samples thus can be limited. Silica glass or ceramics have often been used for both solid and liquid metal samples and organic materials, and a sophisticated ceramic to metal seal used in high-temperature NMR has been described.[3,4] Containers made of tubular single crystals of sapphire (Al_2O_3) are included in this category and can withstand pressures as high as several hundred bars.[5] Silica glass tubes have also generally been used for molten salts, although alkali vapors in particular can cause devitrification and failure at high temperature. Hexagonal

boron nitride, maintained in an inert or reducing atmosphere, has proven to be successful for highly corrosive liquid silicates.[6] Container problems were entirely eliminated by gas-jet levitation in a remarkable new laser-heated probe design.[1]

NMR studies of metals are decreased in sensitivity by the shallow penetration depth of the rf excitation field into good conductors. Greater signal strength, and more predictable rf response, are usually obtained by the use of thin foils or powders dispersed in insulating matrices, which again must be nonreactive. This strategy may become less effective for liquid metals, where drop coalescence may lead to the formation of large particles or even complete separation from the matrix. This problem has been studied in detail,[7] and may not pose difficulties in relatively poor conductors.

High temperatures often generate high vapor pressures, requiring the use of either a sealed, strong sample container or the placement of sample and rf coil inside of a gas pressurized vessel. Because high-pressure NMR is reviewed elsewhere in this issue,[8] we simply note here a number of combined high-pressure and high-temperature designs.[9-12]

Because of the inherently low sensitivity of NMR compared to many other forms of spectroscopy, the reduction in the difference in population between excited and ground states ($N_a - N_b$) caused by thermal energy is a particular problem. The ratio of the populations can be calculated from the Boltzmann equation

$$N_a/N_b = e^{-\Delta E/k_B T} \quad (1)$$

and a good approximation to the population difference is

$$N_a - N_b \approx N_{tot}\Delta E/2k_B T \quad (2)$$

The signal-to-noise ratio ψ, proportional to this difference, will thus be reduced from its room temperature value by a factor of 6 at a temperature of 1500 °C by this effect alone. This reduction in ψ is often at least partially compensated for, however, by reduced line widths caused by increased mobility in both solids and liquids, and, sometimes, by reduced T_1's.

Temperature measurement and control in NMR experiments is complicated by the need to isolate thermocouples from perturbations by and of rf excitation pulses, and to prevent the introduction of spurious noise into the receiver. This generally means location of the temperature sensor at some distance from the sample, requiring the careful calibration of temperature gradients. Optical pyrometry is a useful alternative to thermocouples, particularly above 1600 °C.

Resistive heating elements must meet several unusual design criteria, as reviewed briefly.[3,13] They must be noninductively wound to prevent distortion of the magnetic field at the sample, which can be a daunting task if lines of 1 Hz or less in width are to be observed. A number of geometries have been discussed, including bifilar solenoids, straight wires or rods parallel to the magnetic field, and concentric sheet metal cylinders.[14-16] The latter two approaches have the advantage of keeping most current flow parallel to the field, reducing the rather large magnetic forces on the windings that can result. In some cases, power supplies have been cycled on and off in synchronization with rf pulses to eliminate field perturbations. Generally, DC power supplies are required to eliminate potentially destructive vibrations. Heaters can be placed at a distance from the sample, with heat transfer via a flowing gas stream, as is done in most commercially available probes operating up to 150–250 °C. This technique rapidly becomes inefficient at higher temperatures because of low gas heat capacities, but has been used with success to 600–750 °C in both designs for static probes[3,17,20] and in a new design for an MAS probe.[21] The space available for heating systems in high-field magnets is restricted, particularly in high-field superconducting solenoids. A number of designs have been described for use in electromagnets with parallel pole pieces,[17,22-29] and a few for superconducting solenoids.[14,16,30-32] Designs for flow-through reactor systems inside of NMR probes have begun to allow in situ NMR measurements during realistic catalytic conditions.[33,34] As mentioned above, laser heating can eliminate many of the difficulties of resistive heating.[1]

In most of the designs mentioned so far, the rf coil is close to the sample and is thus close to the sample temperature. This poses a number of additional problems. Thermal noise in the coil wire reduces ψ. The electrical resistivity of metals increases substantially with increasing temperature (often by a factor of 4 from 25 to 1200 °C), reducing the quality factor Q and thus lowering both the excitation field and the sensitivity to the NMR signal. Many of these effects are described in detail in several well-known descriptions of ψ and probe design.[35-37] Equation 1 from the latter reference[37] summarizes what is important:

$$\psi = k\eta M_0(\mu_0 Q\omega_0 V_c/4FK_B T_c\Delta f)^{1/2} \quad (3)$$

Here, k is factor near to 1 dependent on the shape of the coil; η the ratio of the sample to coil volumes, or the "filling factor"; M_0 the nuclear magnetization; μ_0 the permeability of free space; Q the quality factor of the coil; ω_0 the Larmor frequency; V_c the volume of the coil; F the noise figure of the preamplifier; and Δf the bandwidth of the receiver. Fortunately, both the coil temperature term T_c and Q are raised to only the $^1/_2$ power. It is also important to note that the Helmholz coil geometry, required by long sample tubes in standard high-field superconducting magnets, reduces ψ by a factor of about 3.[36]

A fairly typical high-temperature probe design, that has been used primarily for oxides and silicates to temperatures up to 1300 °C, is shown in Figure 1. Various versions of this design have been in use at Stanford for several years, often with a Mo solenoidal rf coil, Mo heating element, and horizontal BN sample tube instead of the Helmholz arrangement illustrated. That shown in the figure can contain the sample in a gas atmosphere different from that used to protect the refractory metals of the heating element and rf coil, an important feature for studies of many oxide phases at high temperature. The upper temperature limit has generally been set by the reduced Q, which limits rf power and sensitivity.

A somewhat similar design is shown in Figure 2. This type of probe has been used for a number of years to study a variety of oxides at temperatures as high as about 1700 °C in a controlled oxygen atmosphere. Measurements of temperature effects on electric field gradients and relaxation times from this group are

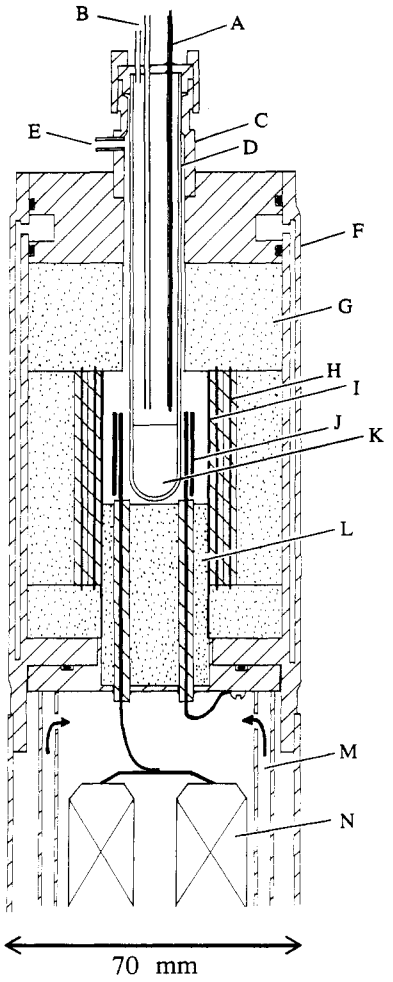

Figure 1. High-temperture NMR probe for superconducting solenoidal magnet. Drawing is somewhat schematic: details such as heating element power leads and control thermocouple, furnace gas inlet, water cooling connections, some thermal insulation, etc., have been omitted for clarity. The figure is labeled as follows: A, sample thermocouple; B, sample gas inlet and outlet; C, sample tube feedthrough and seal; D, sample tube (silica glass, ceramic, etc.); E, furnace gas outlet; F, brass water jacket; G, ceramic fiber insulation; H, heating element (double layer of vertical refractory metal wire in ceramic tubes); I, refractory metal rf shield; J, rf coil (Helmholz design in this configuration may be replaced with solenoidal coil for small, horizontal sample tubes); K, sample; L, ceramic fiber board coil support; M, cooling air tube; N, high power tuning capacitors.

discussed in several sections below, including IV.A. and X.E. The probe, designed to fit into a standard "wide bore" superconducting NMR magnet, is heated by a tantalum wire element that is isolated from the atmosphere of the sample and rf coil by an alumina tube. The element and refractory metal heat shield are maintained in a vacuum to enable extreme temperatures to be reached. A detailed description of the probe and the apparatus for precisely controlling oxygen partial pressure has been recently published.[31]

One obvious solution to the performance problems of a hot rf coil is to maintain it at low temperature. The difficulty here lies in the increase in the ratio of the coil volume to the sample volume ($1/\eta$) that results from the introduction of insulation or dewars between sample and coil. This can often at least in part be compensated by increasing the rf power level, although this is not always feasible for a given probe geometry and spectrometer. In fact, a relatively unappreciated alternative

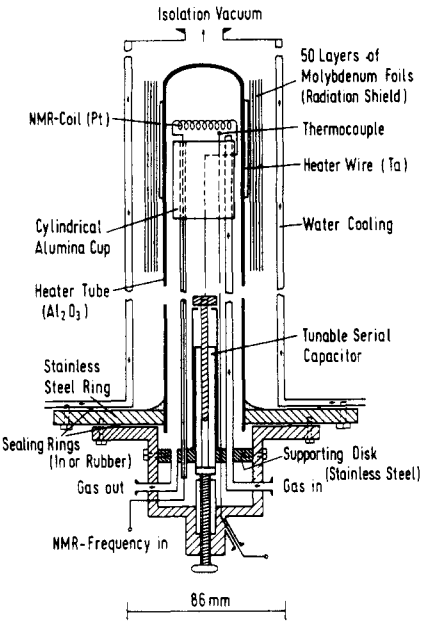

Figure 2. Schematic drawing of high-temperature probe capable of operating to about 1700 °C with sample in a controlled atmosphere (reprinted from ref 31; copyright 1990 Academic Press).

formulation of the above equation (eq 16 of ref 35) shows that if the same rf field strength can be maintained, and the same sample volume is used, ψ for a larger coil is decreased only by the increasing thermal noise of a longer coil wire (which in a cold coil would be lower than in a hot coil):

$$\psi = k\omega_0(B_1)_{xy}M_0V_s/(8K_BT_cR\Delta f)^{1/2} \qquad (4)$$

Here, symbols are as above, with $(B_1)_{xy}$ the rf field strength and R the resistivity of the coil.

A number of designs have used relatively large coils surrounding both heater and sample, and kept cool by insulation or vacuum dewars.[29,38] A compact and potentially very useful new design uses a thin, water-cooled copper tube as the rf coil (Figure 3).[39] This probe has been used to well over 1000 °C and fits within a standard, "narrow bore", superconducting NMR magnet. High-temperature ^{17}O spectra on oxides are described in section IV.A. In all such designs with cooled rf coils, care must be taken to maintain homogeneity of sample temperature within the deliberately imposed large thermal gradients. Heater construction must limit shielding and distortion of the rf signal. Spurious rf noise from the power supply or lead wires must also be minimized.

A number of unusual designs have attempted to circumvent some of the compromises between hot and cold rf coils. Rapid shuttling of the sample between a heater and a cooled rf coil has proven to be useful,[6] but made measurement of temperature and of time dependent phenomena such as relaxation rates difficult. Surprisingly, rf power itself (even from a normal spectrometer decoupler channel) can be used to generate rather high temperatures during an NMR observation, if the rf susceptor is thin enough not to shield the signal from the receiver coil.[40]

The technique of magic angle spinning (MAS) has recently grown to be of great importance in high-resolution spectroscopy of solids, particularly organic compounds and silicates. Making an MAS probe work at

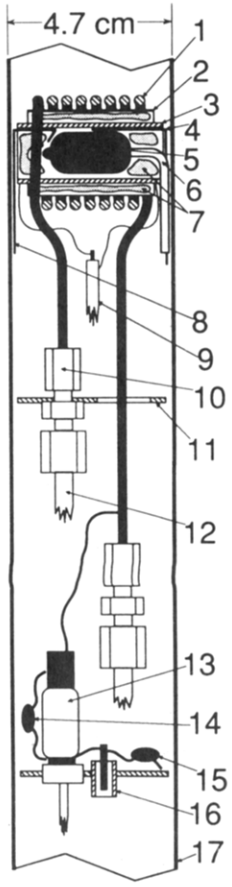

Figure 3. High-temperature NMR probe with water-cooled rf coil: 1, copper tube rf coil; 2, silica glass furnace shell; 3, annular heating element; 4, sample thermocouple; 5, sample; 6, silica glass sample tube; 7, alumina fiber insulation; 8, control thermocouple; 9, coaxial furnace power lead; 10, brass fitting; 11, support plate; 12, teflon water line; 13, tuning capacitor; 14,15, fixed capacitors; 16, BNC connector; 17, cylindrical brass probe body (reprinted from ref 39; copyright 1990 American Institute of Physics).

elevated temperatures is a great technical challenge. New probes, some of which that are commercially available, have recently raised the MAS limit from 250 °C to as high as 600–700 °C.[21,41–45]

Finally, we note a few high-temperature applications of NMR to measurements other than the usual spectra and relaxation studies. Spin echo, pulsed field gradient diffusion measurements have been made in both liquid metals and in molten salts and are described below. Probes for such measurements to 1000 °C have been described.[46,47] A temperature-jump NMR apparatus shows promise for the determination of many rate processes, including structural relaxation and chemical reactions.[48] A spin-projection (1-D imaging) technique has recently been used to measure gas densities at over 300 °C,[50] and high-temperature imaging, especially of liquid–liquid, liquid–solid, or gas–solid mixtures, must soon follow.

III. Applications to Organic Systems

Most NMR studies of organic compounds have been made at temperatures below the range described here, because of the relative thermal instability of complex organic molecules. In several cases, the mobility (and increased spectral resolution) induced by the heating of relatively insoluble synthetic polymers has motivated experiments well above 200 °C.[40,41,50–52] The latter study included well-resolved MAS spectra for both ^{1}H and ^{13}C. In the following sections we focus on the changes that can take place on heating of complex natural polymers to temperatures up to about 600 °C, and on catalysis.

A. Coal and Other Fossil Fuels

Many NMR studies of coal and other fossil fuels have been made, and have been reviewed recently.[53] One common application is of ^{1}H and ^{13}C NMR to characterize the relative proportions of aromatic and aliphatic carbon in coal at room temperature. When coal is heated, a variety of transformations occur that may include the formation of a liquid phase, the loss of volatiles, and eventual carbonization. Because of the large number of different molecular species that are present, NMR spectra are typically poorly resolved. Nonetheless, studies of dynamics (particularly of ^{1}H) and of the abundance of magnetic centers can provide useful clues as to the nature of these changes. T_1 or T_2 data are generally most informative. As summarized in a recent review,[54] the results of heating of coal can include crystal- and glass-to-liquid "melting", covalent bond breaking that produces paramagnetic species, and redistribution of hydrogen. The interaction of water with brown coal (important in understanding the mechanism of industrial drying processes) has been characterized by ^{1}H relaxation studies.[55] Softening and solidification reactions under both oxidizing and inert atmospheres have been studied.[56–59] In situ ESR and NMR results have been gathered on the same sets of samples to allow correlation of abundances of free radicals produced by bond breaking with the mobility of hydrogen.[60–62] The actions of various catalysts on the coal liquefaction process has been observed at high temperature with both organic solvents and a 100 bar pressure of H_2 gas as hydrogen sources.[60,61] Some similar work has been done on oil shale.[63]

B. Pitch

A useful product of both coal and petroleum tars is the complex mixture of polyaromatic hydrocarbons known as pitch, which is a common starting material for the growth of carbon fibers now so important in the composite industry. One of the more intriguing aspects of this process is the development of highly anisotropic, graphitic material from the amorphous precursor, through an intermediate liquid-crystallike "mesophase".[64] Typical ^{1}H NMR results are shown in Figure 4. Here, no spectrum is seen at low temperature because all H is in immobile sites in the glassy solid. As mobility increases at higher temperature, two relatively narrow lines are resolved which represent aromatic and aliphatic H. Further heating, volatile loss, and carbonization result in resolidification and line rebroadening.[65] The relatively high mobility of the soluble, less polymerized fraction of the material is retained at high temperature. Other studies have found both temperature and pressure effects on the aliphatic to aromatic ratio, which decreases as the carbonization proceeds.[66,67] As for coal, complementary ESR and ^{1}H studies have proven useful.[68] ^{13}C NMR spectra on pitch liquids have recently recorded at over 400 °C, despite

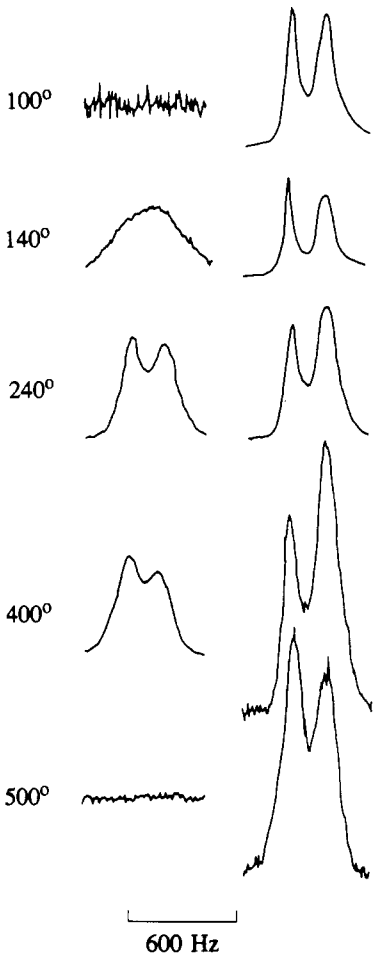

Figure 4. ^{1}H NMR spectra for a coal tar pitch (left) and the fraction of the pitch soluble in both benzene and hexane (right) (reprinted from ref 65; copyright 1988 Butterworth-Heinemann Ltd).

relatively broad lines and the low natural abundance of this isotope.[69]

C. Catalysis

NMR studies of heterogeneous catalysis have been made both at high temperature and on the quenched product of high temperature reactions. In situ studies can eliminate the complications of back-reactions and structural rearrangement during cooling. However, if reaction or exchange rates are sufficient to cause motional averaging, identification of molecular speciation at high temperature may be difficult.

$ZnCl_2$ and $SnCl_2$ catalysts are important in coal liquification and were included in some of the studies mentioned above.[60-62] A number of NMR studies of homogeneous catalysis in flow-through reactors at ambient temperature have been made; recently, the dehydration of 2-propanol in contact with a zeolite heterogeneous catalyst has been observed by ^{13}C NMR to about 180 °C.[34] Other reactions on zeolites in the 150–250 °C range have been observed by MAS NMR,[70,71] including the structure and dynamics of alkoxide intermediates formed from acetylene[72] and the cracking of propene oligomers.[73] Difficult technical problems with rapid spinning of sealed containers of catalyst, liquid and gas phases may be encountered.

The effects of elevated temperatures and adsorbed organic molecules on cation mobility in zeolites has been studied by ^{7}Li NMR.[74] Changes in the aluminosilicate framework with adsorption at elevated temperature have been detected by ^{29}Si MAS.[75,76] Other structural studies of zeolites are described in the next section.

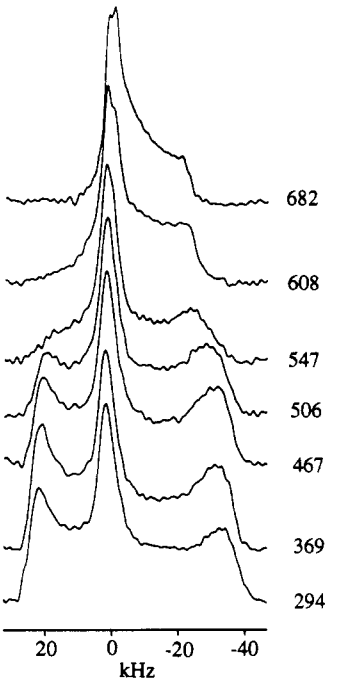

Figure 5. ^{23}Na NMR spectra of dehydrated zeolite K_6Na_6–A. Temperatures in kelvin are shown (reprinted from ref 18; copyright 1989 American Chemical Society).

IV. Silicates and Oxides

In the last decade, solid-state NMR spectroscopy has become an essential tool for the investigation of the local structure of crystalline and amorphous silicates and oxides at room temperature. Applications to these systems at high temperature have been more limited, in part because of the relatively low sensitivity of experiments on several of the most important nuclides of interest (e.g. ^{29}Si and ^{17}O). More work has of course been done on isotopes of higher natural abundance and Larmor frequency, particularly ^{7}Li, ^{11}B, ^{19}F, ^{23}Na, and ^{27}Al.

NMR at high temperature has been useful in characterizing the dynamics of a number of oxides and silicates.[77] Studies of some of these materials are described here, some in sections VI and VII. Crystalline and amorphous ionic conductors, in which either cation or anion mobility is particularly high, have been particularly well studied and are described in section V.

A. Crystalline Phases

If multiple sites produce complex NMR spectra, high-temperature line-shape studies can often provide detail on both structure and dynamics. Zeolites, for example, are framework aluminosilicates of great importance as high-temperature catalysts and catalyst supports. Changes in structure and dynamics with temperature may have important effects on their chemical properties. For example, the ^{23}Na spectrum of dehydrated zeolite Na–A (Figure 5) is the combination of two quadrupolar powder patterns from several

Na sites in the structure: a narrower line from sites with a small electric field gradient (EFG) is superimposed on a broad doublet from sites with a relatively large EFG.[18,19,78] At high temperature, considerable narrowing of the latter was observed. Two dimensional spectral at temperatures of about 400 °C clearly showed a lack of exchange among sites and thus indicated that the narrowing was the result of symmetry changes and a phase transition. Other high-temperature NMR experiments on zeolite-containing systems have been described in section III.C.

The motion of weakly bound alkali cations in silicates can have dramatic effects on the anisotropy in chemical shift (CSA) for ^{29}Si. In Li_4SiO_4, as motion becomes rapid with increasing temperature, all Si–O bonds for the isolated SiO_4 tetrahedra become magnetically equivalent, resulting in a liquid-like ^{29}Si NMR line in a still-crystalline (and nonrotating) solid.[79] This result is analogous to those described below for alkali sulfates: Li_4SiO_4 is indeed the relatively poorly conducting end member of a series of solid solutions with sulfates.[80]

Structural changes with temperature have been studied in several oxides by using ^{17}O NMR, including yttria-stabilized zirconia and the perovkite $BaBiO_3$.[39] In the latter, the disappearance of a broad quadrupolar powder pattern was attributed to the transition to cubic symmetry above 350 °C.

The wealth of orientational information available from single-crystal spectra, as well as the high sensitivity that results from narrow single-crystal lines, was exploited in a ^{47}Ti and ^{49}Ti NMR study of TiO_2 under controlled oxygen pressure at temperatures as high as 1200 °C.[81] In that study, large changes with temperature in the asymmetry of the electric field gradient at the Ti site were linked to the anisotropic thermal expansion of the material. No suggestion of motional averaging was seen. However, in ^{27}Al spectra of Al_2O_3 dissolved in TiO_2, some kind of motional effect caused line broadening and signal disappearance at high temperature,[82] possibly related to exchange involving defect or interstitial sites. Detailed relaxation time studies of cation and defect motion in TiO_2 and other phases are described in section VI.

MAS studies, which can provide greatly enhanced resolution and sensitivity for polycrystalline or amorphous samples, have only recently become possible at high temperature. Zeolites often show multiple ^{29}Si MAS resonances. In several studies to about 150 °C, multiple ^{29}Si MAS lines coalesced at elevated temperature, either because of dynamical configurational change or static symmetry increase.[75,76] The crystallization of an aluminum phosphate zeolite from an aqueous gel was observed in situ to about 150 °C.[83] A recent MAS study to 500 °C of cation motion in the framework silicate nepheline ((Na,K)$AlSiO_4$) (Figure 6) also showed the utility of this technique.[43] In this material, Na cations are located in two sites, which in the MAS spectra are quite distinct. As the sample was heated, the initial effect was a sharpening of the two individual quadrupolar doublets, presumably because of increased intercage motion. At higher temperature, diffusion among sites became rapid compared to the frequency separation of the two lines, and motional averaging was observed. The estimated rate of exchange of Na between two inequivalent sites was close to that expected from conductivity and bulk diffusion measurements.

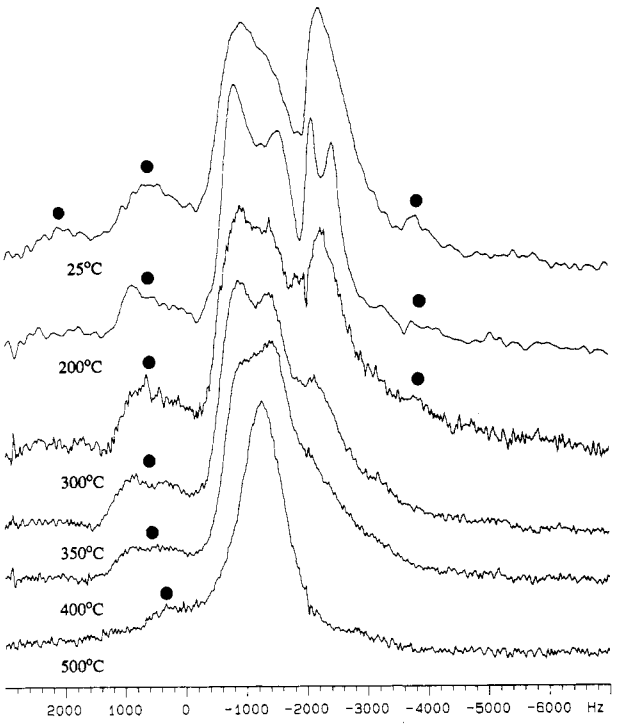

Figure 6. ^{23}Na MAS NMR spectra of synthetic nepheline ($Na_{0.75}(Na_{0.20}K_{0.05})AlSiO_4$) at high temperature. Spinning side bands are marked by solid circles.

B. Glasses and Liquids

In oxide liquids of relatively low viscosity (either because of composition or temperature), fully exchanged, narrow-line liquid spectra are generally observed. For ^{27}Al in a number of aluminate liquids (studied at temperatures as high as 2100 °C in a laser-heated, gas-levitated sample), for example, single peaks are observed whose positions indicate the relative proportions of Al with four or six oxygen neighbors.[84,85] In a variety of silicate liquids, single narrow ^{29}Si lines are present,[6,32,79,86–88] again indicating rapid exchange among a variety of structural species known to be present from NMR studies of glasses and from high-temperature vibrational spectroscopy. This finding was somewhat surprising in silicates in light of theoretical treatments based on polymer theory, but seems to correspond qualitatively to the results of molecular dynamics simulations.

The excellent glass-forming ability of some silicate liquids has allowed structural mobility to be explored in detail by high-temperature NMR line shape studies. As shown in Figure 7, for example, the ^{29}Si line shape for $K_2Si_4O_9$ liquid just above the glass transition temperature is a composite of a narrow central peak for symmetrical Si sites with four oxygens bonded to Si neighbors (Q^4), and a broader uniaxial pattern for Si sites with three oxygens bonded to Si and one bonded to Na (Q^3). With increasing temperature, these sites begin to exchange, eventually resulting in complete motional narrowing. This process can be modeled to obtain exchange frequencies. Because this exchange involves breaking the strongest bonds in the system (Si–O), it is likely that this process is closely related to transport properties and to configurational entropy.

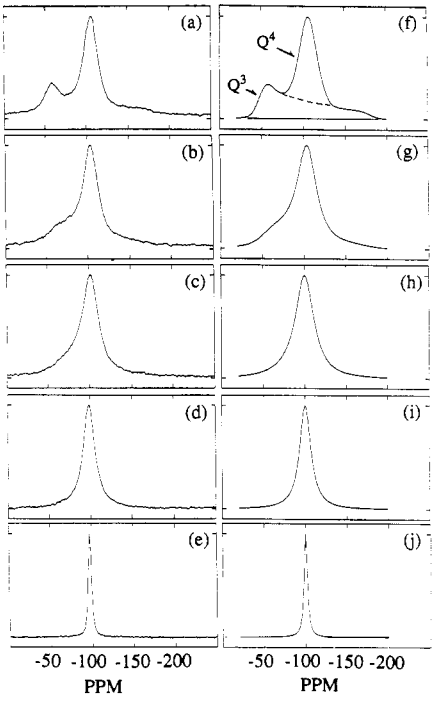

Figure 7. ^{29}Si NMR spectra (a–e) of $K_2Si_4O_9$ liquid and simulations from a multisite exchange model (f–j). The contributions from the two dominate local structural units are labeled in f (see text). Spectra were recorded at the following temperatures: a, 697; b, 774; c, 800; d, 847; e, 997 °C. Simulations were made with the following exchange rates: f, 2000; g, 10 000; h, 25 000; i, 50 000; and j, 500 000 Hz. Results are described in detail in ref 79.

This has indeed been demonstrated: bulk viscosity can be directly calculated from species exchange rates measured by NMR.[79] The exchange among Si sites is mirrored by that among O sites: ^{17}O NMR has shown that bridging and nonbridging oxygens interchange at rates comparable to that of the Si sites.[89] This kind of study has been extended to temperatures just above T_g by two dimensional exchange spectroscopy.[90] This kind of structural exchange is in marked contrast to the behavior of a mixture of molten alkali nitrate and sulfate, where no exchange among the oxygens bound to these molecular anions was observed.[1]

A few relaxation time studies of network forming species in oxide glasses and liquids have been made, with some early high-temperature relaxation time results, on ^{11}B in B_2O_3.[91,92] ^{29}Si data in glassy and liquid silicates have proven difficult to understand in complete detail, in part because of the sensitivity to paramagnetic impurities.[79,88] However, relaxation mechanisms change abruptly near the bulk glass transition temperature, probably because of the structural mobility that begins at that point.[79,88] Apparent activation energies in the liquid region are similar to those for viscosity. The detection of T_1 minima gave, in some cases, good constraints on correlation times.

Anion motion can be particularly high for F^- in fluoride-containing glasses, as can cation motion in alkali-containing glasses. These are discussed in some detail in section V. Behavior at the transition from glass to liquid has been much less thoroughly studied, but is of particular interest in light of results on the dynamics of network forming cations. Spin–lattice relaxation for ^{23}Na in silicate glasses, for example, may be controlled by local cation "rattling" motions at relatively low temperature (resulting in relatively low apparent activation energies), but as the glass transition temperature T_g is approached, diffusion among sites becomes rapid enough to dominate. Under these conditions, E_A for the relaxation process becomes equal to that for bulk diffusion.[88] In the latter study, a minor inflection in the T_1 curve at T_g was observed for ^{23}Na in several silicate glasses, indicating some relatively weak coupling with the motion of the silicate network.

V. Ionic Conductors

Electrical conductivity in many if not most ionic solids is controlled by the diffusion of either cations or anions. A number of families of materials have been discovered in which, at temperatures far below the structural melting point, this motion and the conductivity become comparable to those of an ionic liquid. This phenomenon has sometimes been described as "lattice melting". These fast- or super-ionic conductors have considerable technological use and promise as solid-state electrolytes and electrodes in high temperature, high efficiency batteries and fuel cells, and in gas pressure and chemical sensors (e.g. oxygen monitors in automobile engines). Many NMR studies of these materials have been made, and have been previously reviewed.[93–98] Recent work at high temperature will thus be emphasized, with some illustrative earlier examples. In a number of materials, the transition to the high conductivity state is accompanied by significant structural effects, and these are thus described below in the section on phase transitions.

NMR studies of a number of high-temperature ionic conductor systems are especially convenient because the mobile ions have high natural abundance and relatively high Larmor frequencies, for example ^{19}F, ^{7}Li, and ^{23}Na. As in other materials, both line-shape and spin–lattice relaxation studies have been useful. Interpretation of the latter is not always straightforward, however. In particular, local ionic motion can dominate T_1 behavior, sometimes making difficult the assessment of bulk diffusion (usually the property of primary interest). Studies using multiple isotopes, pulsed field gradient techniques, or measurements at two or more widely separated magnetic fields are among the more definitive. NMR has been particularly useful in screening candidate materials and comparing different synthesis procedures: lack of significant ionic mobility usually indicates lack of significantly enhanced conductivity.[95]

A thorough review of the relatively early work in this field discusses in detail the problems of interpretation of relaxation and line narrowing.[97] These complications are not limited to ionic conductors and are similar in some ways to effects described below for liquid metals and molten salts. Divergence from simple BPP models often includes the findings that the apparent activation energy ($d \ln T_1/d[1/k_BT]$) is substantially smaller below the T_1 minimum than above it, and that the low temperature E_A is smaller than that for tracer diffusion or electrical conductivity. The frequency dependence of T_1 at temperatures below the minimum is also not always that predicted by BPP theory. T_2 is often less than T_1, even well above the T_1 minimum, because of extra line broadening mechanisms such as coupling to paramagnetics or the partial averaging of signal from satellite transitions. The dimensionality of diffusion may be reduced to one or two by highly anisotropic

crystal structures, changing the predicted form of the temperature and frequency dependencies of T_1 and T_2. The "attempt frequency" (section I), often estimated from the BPP relation that the jump frequency equals the Larmor frequency at the T_1 minimum, may have little physical meaning if the BPP model is inappropriate.

A common approach to dealing with at least the apparent dependence of E_A on temperature is to derive a model with multiple correlation times or distributions of activation energies. Site exchanges with higher E_A values become more significant at higher temperature as average thermal energy increases. This type of model has often been correlated with multiple sites or exchange mechanisms, as suggested by structural or mechanistic arguments, and has been used in many of the examples described below. However, as has been recently pointed out, "homogeneous" models with single, but nonexponential, correlation functions can sometimes fit the same observations.[99] The most common modified form of the correlation function is $g(t) = \exp[(-t/\tau)^{\beta}]$, with β between 0 and 1. This kind of function has proven to be useful in describing mechanical and dielectric, as well as nuclear spin, relaxation. This approach can have the advantage of increased generality, but may be more difficult to relate to simple physical models of diffusion.

A. Crystalline Anionic Conductors

Experimental systems can be conveniently divided into those where conductivity is controlled by rapid anion diffusion and those where cation motion dominates. A number of fluorides fall into the first category. However, F^- diffusion is difficult to study directly by tracer methods because of the lack of a suitable radioisotope. An early ^7Li and ^{19}F NMR study of crystalline LiF at high temperature showed good agreement in activation energy with bulk Li^+ diffusion results and gave some of the first details of F^- motion.[100] A systematic investigation of the influence of paramagnetic impurities in CaF_2 (fluorite) showed their dominance of T_1 at low temperature.[101] At high temperature, increased F^- ion mobility provided a second relaxation mechanism and caused an abrupt increase in the apparent activation energy, possibly analogous to that described above for ^{29}Si in a silicate transforming from a glass to liquid. A pulsed-field gradient NMR study of F^- in BaF_2 provided an accurate determination of the diffusivity independent of models of the relaxation process.[102]

PbF_2 also has the fluorite structure, but becomes a true "fast ion conductor", with a marked heat capacity anomaly accompanied by a transition to nearly liquid-like conductivity.[103] ^{19}F NMR showed this transition as an abrupt change in the spin–lattice relaxation mechanism,[103,104] and again, pulsed field gradient methods gave an accurate measurement of long-range diffusivity.[103] Paramagnetic impurities (possibly formed by reduction of Pb^{4+} at high temperature) complicated detailed interpretations of relaxation time data. The effects of doping and of disorder in fluorite-structured $K_{0.4}B_{0.6}F_{2.2}$ have also been studied by ^{19}F T_2 measurements.[105]

A series of high-temperature ^{19}F NMR studies have explored the complexities of diffusion and conductivity

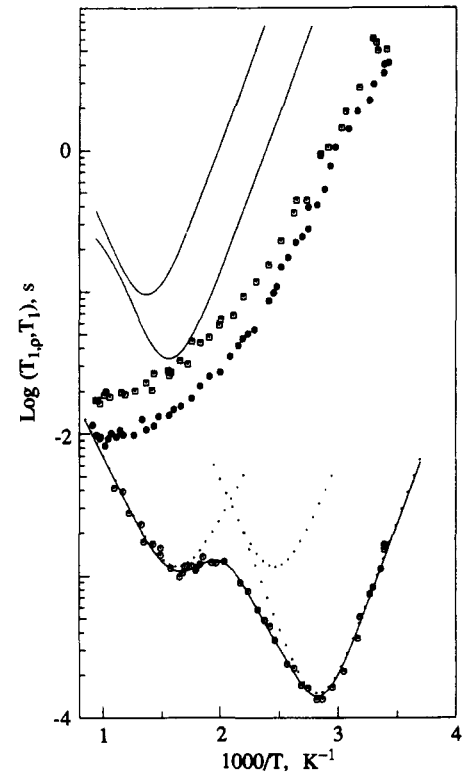

Figure 8. ^{19}F relaxation time data for LaF_3. Upper symbols and curves are T_1: open symbols are data collected at 60.9 MHz, solid symbols at 21.5 MHz; lower symbols are for $T_{1\rho}$ (reprinted from ref 108; copyright 1983 Elsevier Scientific Publishers).

in LaF_3 (tysonite) and related phases, in which F^- ions reside on three distinct sites or "sublattices". Several relatively early studies again showed the complications created by paramagnetics in interpretation of relaxation time data,[106] and the effects of vacancies introduced by solid solution with lower valence cations such as Ca^{2+}, Ba^{2+}, and paramagnetic U^{4+}.[107-111] In this work, as well as a more complete study to about 1000 °C (which included a detailed treatment of F–F dipolar coupling), T_1 and $T_{1\rho}$ results could be explained only by the presence of two dynamically distinct lattices (one presumably combining two of the F^- sites) with separate correlation times.[112] As shown in Figure 8, this gives a clear signature, especially in the slow dynamics sampled by $T_{1\rho}$, where there are two distinct minima. Very recently, a single-crystal study of LaF_3 removed the F–F dipolar broadening through the use of multipulse homonuclear decoupling, enabling detailed line shape interpretation up to about 200 °C.[113]

Fluoride ion dynamics have again been characterized by high-temperature NMR in a new class of fluoride ion conductors, M_2SbF_5 ($M = Rb^+, K^+, Cs^+, Tl^+, NH_4^+$).[114] Three distinct relaxation mechanisms were reported and were again most prominent in the $T_{1\rho}$ measurements. These were related to three types of motion, including coordinated motions of the SbF_5 groups and F^- diffusion.

Oxide anion conducting ceramics are especially interesting as high-temperature solid electrolytes in oxygen pressure sensors. ^{17}O NMR generally requires the use of isotopically enriched materials because of the low natural abundance and Larmor frequency, but a few studies have been made at high temperature. Conduction in CeO_2, for example, is controlled by the

abundance of defects generated by doping with a lower valence oxide such as Y_2O_3. A detailed ^{17}O NMR study of signal intensity, T_1, and T_2 data provided information on defect mobility in this phase.[115,116] As in other systems described above, a large increase in apparent activation energy from the low-temperature to the high-temperature side of a T_1 minimum was well fitted by a model based on a wide distribution of activation energies for site jumping.

B. Crystalline Cationic Conductors

Among cation-conducting solid-state electrolyte materials, one of the best-studied phases is sodium β-alumina, with stoichiometry approximately $Na_2Al_{22}O_{34}$. This material is the most commonly used member of a family of conductors that may contain several other pairs of mono- and trivalent cations.[117] Up to about 25% of excess Na_2O can be added to the structure to enhance conductivity. As previously reviewed,[96] a number of ^{23}Na NMR studies at low temperatures have observed the multiple alkali sites thought to be present from X-ray diffraction studies.[117-120] Mobility is sufficient to average these lines to a single peak at only 110 K.[117] The quadrupolar shape of this peak still indicates an average nonzero asymmetry parameter up to at least 200 °C, however, presumably because motion is restricted within a two-dimensional sheet. A single-crystal study to about 800 °C showed a highly asymmetric T_1 minimum, somewhat similar to that described below for alkalis in glasses: the apparent activation energy increases by a factor of about two with rising temperature.[121] Models with a wide distribution of energy barriers (activation energies) could reproduce the data, and some evidence for a bimodal distribution of barriers was seen: local motion may dominate at low temperature, through going diffusion at high temperature. Some correlation between the defect density introduced during sample synthesis and the relaxation behavior was noted. The inapplicability of single exponential correlation functions was also noted in work on the gallium analogue.[122]

Another high-temperature study of a commercial, Li-containing, polycrystalline β-alumina showed similar behavior, except that a new relaxation mechanism caused another T_1 slope break above about 250 °C.[123] This study also emphasized the difficulties of uniquely interpreting T_1 data for a quadrupolar nucleus and showed the great sensitivity of derived frequency factors to assumptions about the relaxation process. The relaxation behavior of ^{23}Na in a "Nasicon" phase ($Na_3Zr_2PSi_2O_{12}$) was generally similar to that of β-alumina.[123]

Possible cation substitutions in β-aluminas also include relatively labile protonated species, including NH_4^+, H^+, and H_3O^+. In at least the last case, some protons remain in the structure to at least 500 °C, and their mobility has been studied by ^1H NMR.[124]

Spin-lattice relaxation of the relatively immobile cation Al^{3+} in β-alumina is also controlled by Na^+ motion, as shown in a single-crystal ^{27}Al study.[125] This work suggested that because this nucleus is apparently less sensitive to local motions, it might actually be a better probe of long-range dynamics than ^{23}Na. Good agreement between the correlation time at the T_1 minimum and that estimated from Na bulk diffusivity was demonstrated.

The small size of the Li^+ cation makes it a highly mobile species in a variety of solids, as mentioned above for Li_4SiO_4. Following earlier line-narrowing studies,[126] T_1 and line shape data for ^7Li in "Lisicon" ($Li_{16-2x}Zn_x(GeO_4)_4$) ionic conductors, for example, indicated long-range diffusion with a high activation energy.[127] An Li "Nasicon" phase ($LiZr_2(PO_4)_3$) shows rapid Li^+ motion and ^7Li line narrowing above 280 °C.[128] ^7Li lines narrowed at even lower temperatures in a variety of borate, phosphate, and silicate ionic conductors.[80] ^7Li T_1 data have also been collected at elevated temperature in the intermetallic ionic conductor LiAl.[129]

Work on both ^7Li and ^6Li in Li_3N provided detailed constraints on cation motion, suggesting a change from intralayer mobility at low temperature to interlayer hopping at high temperature, accompanied by a change to liquid-like line shapes.[130,131] Other studies at high temperature on this phase have included ^{14}N measurements[132] and the effects of solid solution and intermediate compounds in the Li_3N–LiCl system.[133]

Li^+ conductivity in LiI can increase by up to 1000 times when the material is mechanically mixed with an "inert" powder such as Al_2O_3 or SiO_2.[134] This odd phenomenon was correlated with a two-component spin–lattice relaxation time for ^7Li, with the fast component attributed to interface sites.[134] Further work on single crystals and dispersed powders included pulsed field gradient diffusion measurements and extremely pure starting materials.[135,136] Similar effects in dispersed LiCl have also been noted.[137]

In the one-dimensional conductor phase of β-eucryptite (β-$LiAlSiO_4$), ^7Li T_1 behavior was similar to that of ^{27}Al.[138] However, relaxation was nearly independent of the observation frequency, indicating that a standard BPP model was not applicable. Apparent T_1 minima were therefore interpreted as a change in relaxation mechanism related to the known transition from ordered to disordered Li positions in the structure. Further studies included a more detailed model of one-dimensional Li^+ motion as well as 3-D spin diffusion to paramagnetic impurities.[139]

One-dimensional cation motion is also required by relaxation time measurements in the hollandite-structured alkali titanites, or priderites ($A_xB_yTi_{8-y}O_{16}$, where A = K^+, Rb^+, Cs^+, Ag^+, Ba^{2+}; B = Mg^{2+}, Al^{3+}, Cr^{3+}, Fe^{3+}, Ga^{3+}). Early studies used ^7Li NMR,[140,141] while later work used ^{27}Al as a probe.[142,143] The former study found evidence for two structurally and dynamically distinct Ba sites in a Ba–Al priderite, both in the splitting of ^{27}Al single-crystal satellite transitions and in T_1 data.

High-temperature NMR work on a variety of other crystalline ionic conductor has been reported. Some of the numerous studies of pyrochlore phases extend to relatively high temperature, such as ^{205}Tl work on $TlNb_2O_5F$.[144] ^{63}Cu T_1 data on CuI clearly showed the effects of "lattice melting" at the onset of rapid Cu^+ motion well below the real melting point.[145] High Cu mobility has also been detected in several Cu sulfides and selenides studied up to about 300 °C.[146] NMR up to 800 °C characterized alkali mobility in a number of anti-fluorite structures (Li_2S, Li_2O, Na_2S, Na_2O).[147]

A number of NMR studies of ionic conductors (and other systems, especially liquid metals) have been made by using "nuclear" techniques instead of conventional NMR spectrometers. This work largely falls outside the

scope of this review, but will be mentioned here for completeness. In this approach, short-lived radionuclides are generated in a sample by bombardment with a beam of particles from a nuclear reactor or accelerator, in the presence of a magnetic field to polarize nuclear spins. The radiation emitted is anisotropic, and the decay with time in the anisotropy measures the spin–lattice relaxation rate. As described in a recent lengthy review,[148] one of the more commonly employed reactions is the neutron activation of ^7Li to form ^8Li, whose β radiation is detected. This technique has been used to study relaxation dynamics and diffusion of Li in a wide range of materials at ambient and high temperature, including LiC_6,[148] Li_3N,[149] and a number of liquid Li alloys described in section X.

C. Amorphous Ionic Conductors

Diffusion and ionic conductivity in amorphous materials has much in common with the crystalline phases discussed above, and theoretical approaches have often been similar. Constraints of well-known structure are often absent, but effects of anisotropy are not likely to be significant, at least in bulk samples. One recent model of the theory of relaxation in glasses is based on a specific hopping model for diffusion, instead of relying on generalized equations for correlation times.[150] Another very recent approach emphasizes the fundamental difference between glasses and liquids or crystalline solids: the former are not in thermodynamic equilibrium. Their response to a time-dependent perturbation, such as an NMR signal, may thus be strongly frequency dependent.[98] A remarkable similarity between frequency-dependent electrical conductivity and the typical non-BPP T_1 behavior was noted: the commonly observed low values of E_a at low temperature may be the result of structural relaxation effects.[98]

In alkali silicate, borate, and phosphate glasses, the motion of the alkali cations largely controls the conductivity and dielectric properties. As in other materials, nuclear spin relaxation time studies in glasses have provided important constraints on models of both local and through-going diffusive dynamics.[151] Results from one extensive study[152] are shown in Figure 9. Here, the observation of maxima in $1/T_1$ provided quantitative constraints on correlation times for the motion of Li^+ cations in the glasses, and temperature slopes gave information on activation energies. The increase in the apparent activation energy from just below to just above the maximum in $1/T_1$ is a good example of deviation from typical BPP behavior. In several studies of phosphate, borate, and silicate glasses the observed apparent activation energies derived from Arrhenius plots of T_1 data are usually well below those for electrical conductivity or cation bulk diffusion, suggesting multiple correlation times or distributions of activation energies.[152-155] $T_{1\rho}$ data also provided constraints on much slower motions. ^7Li T_1 data has been measured up to about 200 °C in the sulfide analogues of lithium silicate glasses (Li_2S–SiS_2 system),[156] and ^8Li spin–lattice relaxation in lithium borate glasses has been measured by β-detected NMR in a similar temperature range.[157]

Ag^+ mobility creates high ionic conductivity in a number of AgI-based systems, both crystalline and glassy. Several ^{109}Ag NMR studies of these materials have been made. A few of these extend into the 200–300 °C range, including work on borate-containing glasses[158] and systems with sulfide.[159]

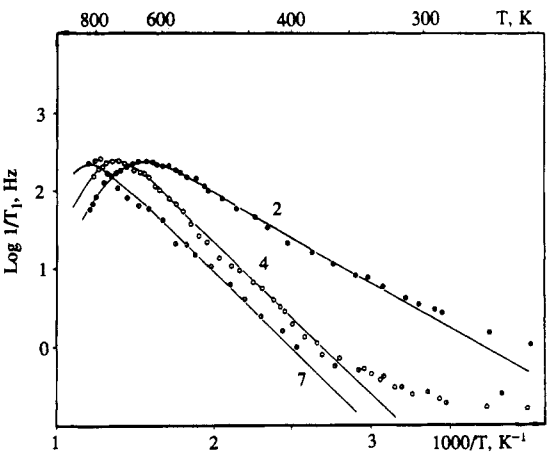

Figure 9. $1/T_1$ data for ^7Li, plotted against inverse temperature, for glasses of compositions $Li_2Si_2O_5$ (curve 2), $LiNaSi_2O_5$ (curve 4), and $LiKSi_2O_5$ (curve 7). Solid lines show results of a model fitted to high temperature data (reprinted from ref 152; copyright 1979, Academic Press).

As in crystalline fluorides, increased mobility and narrowing of the ^{19}F resonance has been observed in a number of fluoride-containing glasses at high temperature.[14,155,160] Glasses based on ZrF_4 are especially interesting as optical waveguide materials with very low loss in the infrared.[160]

VI. Defects in Ionic Crystals

Vacancies and other kinds of defects control diffusion in many of the materials already described and will also be discussed for metals in section X. Here we describe high-temperature NMR work on defects in a number of simple salts and oxides. Several relatively recent reviews describe such studies in more detail.[77,161,162]

Impurities can distort crystal lattices enough so that quadrupolar nuclei experience increased electric field gradients as much as five or six atom shells away. Even small amounts of dopants can therefore strongly effect signal intensities, and, if mobile, can markedly reduce relaxation times. Diffusion rates for impurities have been calculated from T_1 data for a variety of salts, requiring, as usual, the assumption of a model of the relaxation and diffusion processes.[163] Similarly, the rate of aggregation of impurities (that may lead to phase separation) can be estimated, as for Ca^{2+} in NaCl.[164] Defects in silver halides are of particular interest because of their importance in photography. Most NMR studies on silver salts have concentrated on subambient temperatures; a few have extended to temperatures above 400 °C, as in investigations of the diffusion of Li and Na impurities in AgBr.[165]

In recent ^{47}Ti and ^{49}Ti single-crystal studies of TiO_2 (rutile) to temperatures as high as 1200 °C, $1/T_{1\rho}$ showed three peaks, indicating three relaxation mechanisms.[166] These data, combined with relaxation after site-selective excitation[162] and the effects of sudden changes in oxygen pressure, enabled four types of motion to be distinguished, including that of Ti^{4+} itself, Fe impurities, Al or Cu impurities, and oxygen vacancies. Similarly elegant results were obtained for ^{47}Ti and ^{87}Sr NMR on $SrTiO_3$ to about 1500 °C.[167]

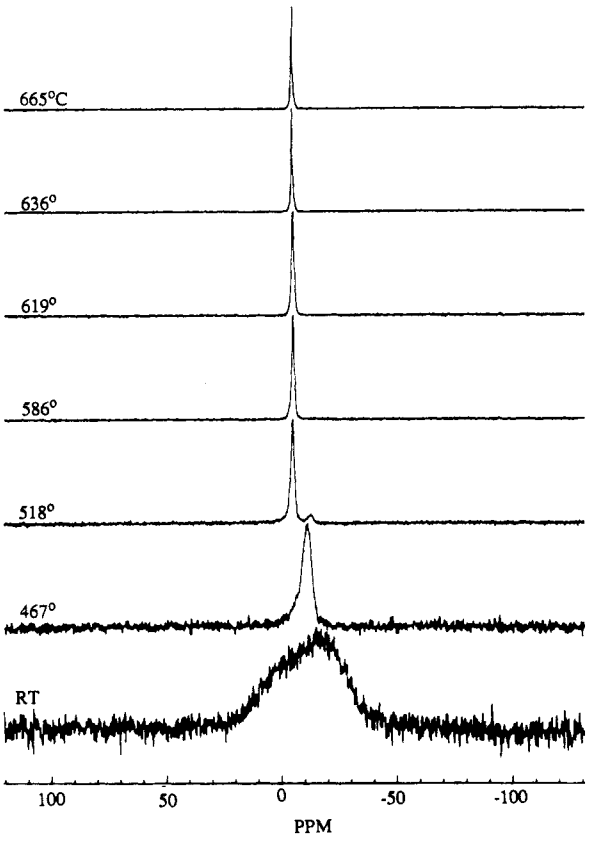

Figure 10. High-temperature ^{23}Na spectra for $LiNaSO_4$. At 518 °C, most of the sample has transformed to the superionic conductor phase. Above 620 °C, the material is completely molten and shows a further decrease in line width (reprinted from ref 172; copyright 1990 Elsevier Scientific Publishers).

The motion of dislocations, and the blocking of such motion by various kinds of defects, is the primary control of the strength of many types of materials undergoing plastic deformation. In technically challenging studies, the motions of dislocations during mechanical strain of ionic crystals and polycrystalline metals has been studied by NMR at both low and high temperature, and as functions of impurity content.[161,168-171] In those studies, the sensitivity of $T_{1\rho}$ measurements to slow motions was again exploited: relaxation can be greatly enhanced during deformation. The average jump distances and times, as well as the concentrations, of mobile dislocations were all quantified.[161]

VII. Phase Transitions

Several transitions in crystal structure have been described above for silicates, and melting reactions of organic compounds, silicates, oxides, salts, and metals are described in the appropriate sections. Here we describe high-temperature NMR work on a variety of structural and order–disorder transitions in crystalline inorganic solids.

$LiNaSO_4$ is one of a series of solids in which crystallographic transitions accompany the development of fast ionic conductivity and the apparent rotation of the sulfate groups. At 518 °C the phase transforms from a trigonal to a cubic structure and shows a 1000-fold increase in electrical conductivity. Melting at 620 °C results in a much smaller increase in conductivity. As shown in Figure 10, ^{23}Na line shape data show these

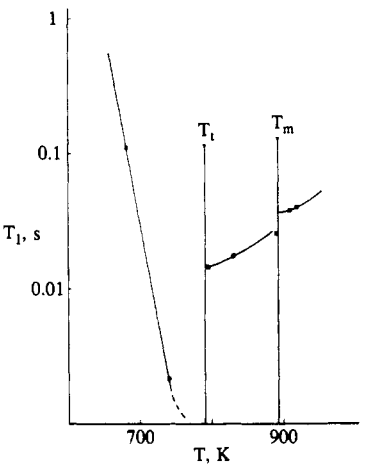

Figure 11. T_1 data for ^{23}Na in $LiNaSO_4$ at high temperature. T_t is the transition point to the superionic conductor; T_m is the melting point (reprinted from ref. 172; copyright 1990 Elsevier Scientific Publishers).

changes clearly.[172] Below the transition, the line gradually narrows. At the transition, a new, narrower line appears. 2-D nutation spectra show that this contains all collapsed satellite transitions, indicating nearly liquid-like motion of the cations. At the melting point, further narrowing occurs. Similar results are seen in ^7Li spectra. T_1 data (Figure 11) show dramatic changes in slope and magnitude at the transition temperature, with smaller effects at the melting point. Other recent relaxation time studies of Li–Na solid solutions highlighted the difference in the dynamics of Na^+ and Li^+.[173]

$KLiSO_4$ also transforms to a fast ion conductor. A recent high-temperature ^{39}K NMR study provided new structural data on the nature of the transition, and allowed estimation of the Li^+ ion diffusion constant.[174] Because single-crystal techniques were used, the poor sensitivity and chemical shift dispersion of this low Larmor frequency nucleus were overcome. Surprisingly, the fast transition on heating of this material involves a *reduction* in symmetry from hexagonal to orthorhombic.

Twenty-six degrees below its melting point of 319 °C, NaOH goes through a first-order phase transition to cubic symmetry with mobile OH^- ions. The relationship between this reorientation and the transition mechanism has been studied by ^1H, ^2H, and ^{23}Na NMR.[175]

In contrast, Na_2CO_3 is not a fast ionic conductor, but it does undergo two symmetry changes at 260 and 490 °C.[176] The ^{23}Na quadrupolar line shape showed a clear decrease followed by an increase in the quadrupolar asymmetry parameter η on heating, but surprisingly, there were no abrupt changes at the transition temperatures.[176]

Recently, NMR has been applied to several high-temperature structural phase transitions in silicates and their phosphate analogues. For example, several polymorphs of SiO_2 and $AlPO_4$ undergo displacive transitions to high-temperature forms whose high symmetry may be due to motional averaging. This can occur even in these strongly bound framework structures by cooperative bending motions or librations of interconnected tetrahedra. Single-crystal ^{29}Si line shapes and T_1 measurements have recently been reported for quartz.[177] ^{17}O and ^{29}Si data for SiO_2 cristobalite,[177] and ^{27}Al and ^{31}P spectra for its phosphate analogue,[178] have

been collected at high temperature, including MAS studies on the latter.

NMR and NQR studies of a wide variety of other structural phase transitions, at low and high temperature and including salts, organic compounds, and oxides, have been thoroughly described in several lengthy reviews.[179,180] The utility of T_1 data for quadrupolar nuclei, as well as measurement of electric field gradient tensors in single crystals, were emphasized, and numerous case studies of both structural and dynamical information were described. A good example is that of measurements to about 900 °C on ^{23}Na and ^{93}Nb in the perovskite phases $KNbO_3$ and $NaNbO_3$.[181] In the latter phase, inflections in the T_1 curve are seen at four transition temperatures. For the highest one, a large effect was attributed to a dynamical disorder in the oxygen atoms. High-resolution, single-crystal study of $NaNbO_3$ clearly showed the relationship between transition-induced changes in the EFG at the Na site, local structure, and bulk properties such as the refractive index.[182]

VIII. Molten Salts

Molten salts are interesting as potentially simple ionicly bound liquids, as well as having a number of technological uses. Once more, NMR studies have contributed greatly to the understanding of both dynamics and structure, as reviewed in part previously.[3,13,183,184] In general, the viscosities of molten salts are lower than those of molten silicates and oxides, and NMR lines are usually fully averaged. Most studies have therefore been of isotopic chemical shifts and relaxation. However, line shape measurements on molten salts somewhat analogous to silicates will first be mentioned.

Molten aluminochloride salts are highly structured liquids of considerable interest as electrolytes in high-temperature batteries. Some aluminochloride systems, particularly those with small organic cations (such as pyridinium and imidazolium), are liquids at or slightly above room temperature, but exemplify the behavior of similar materials at high temperature. In much of the range of compositions explored, the anionic structure of these liquids is dominated by isolated $AlCl_4^-$ molecules and $Al_2Cl_7^-$ dimers. ^{27}Al NMR has detected separate signals for these species[184,185] and has shown that they exchange as temperature increases. Theoretical calculations indicate that the mechanism of exchange involves a transition state of Al with five Cl neighbors,[186] similar to that proposed for species exchange and diffusion in molten silicates.[79]

In contrast to silicates and aluminochlorides in their high viscosity ranges, most molten salts are mobile enough to produce relatively narrow-line, averaged NMR spectra. In some of these systems, however, strongly bound small molecules do seem to persist well above the melting point. In Li_2BeF_4 (proposed as a coolant in nuclear reactors), for example, a detailed T_1 study of both ^7Li and ^{19}F indicated that diffusive motion controls relaxation in both crystal and liquid.[187] The similarity of ^{19}F line shapes in the two phases suggested that BeF_4^{2-} units persist to at least 550 °C in the melt, consistent with X-ray scattering data. The BeF_4^{2-} groups do not seem to undergo free rotation and consequent complete line narrowing, but are apparently somewhat hindered by the formation of larger clusters. BeF_2 melt systems again are analogous in many ways to molten silicates, with significant covalent bonding.

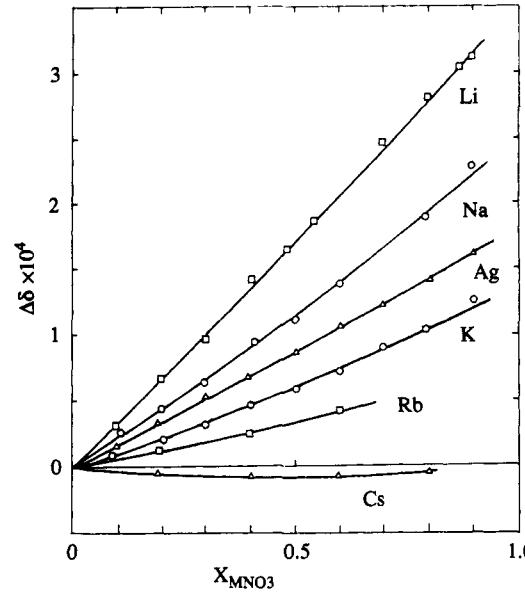

Figure 12. Chemical shifts for the dipolar nucleus ^{205}Tl in molten salt solutions of $TlNO_3$ and MNO_3, where M is a monovalent cation indicated on the figure. Data were collected at 400 °C for the Tl–Cs solutions and at 350 °C for the other compositions (reprinted from ref 188; copyright 1983 American Chemical Society).

Molten salt systems can provide a chemically rather simple view of the influence of structure and bonding on NMR chemical shifts. ^{205}Tl is a convenient spin $^1/_2$ nucleus, and Tl^+ is large and deformable enough to have both a large range in δ and significant covalent bonding. A systematic study of the effect of substitution of other cations in thallous nitrate and chloride melts (Figure 12) demonstrated that chemical shielding systematically increased with decreasing size and increasing electronegativity of the "foreign" ion,[188] confirming much earlier conclusions.[189,190] This behavior was explained by the increase in Tl^+–Cl^- overlap and is consistent with trends in thermochemical data.[188] This relationship between chemical shift and second neighbor cation properties is qualitatively similar to those seen in other systems where the primary contribution to variations in chemical shifts is paramagnetic, including silicates with both four- and six-coordinated Si.[191–193] For a cation X (being observed by NMR), first neighbor cations of increasing electronegativity decrease the covalency of the bond from X to the anion, reduce the paramagnetic deshielding, and lower the resonant frequency. Similar conclusions were reached in work on ^{127}I and ^{81}Br in molten Tl salts.[194] The systematic effect of "softness" of the anion in Tl molten salts was made clear when Tl_2S was added to TlCl,[195] and the effects on ion polarization in molten salt mixtures has been further explored by ^7Li and ^{133}Cs relaxation time studies in molten Li–Cs nitrates.[196–198] Speciation in molten indium chlorides has also been explored by ^{115}In NMR at high temperature.[199]

A variety of studies of other molten salt systems have again provided both structural and dynamical data.[183] For quadrupolar nuclei including ^7Li, ^{23}Na, and ^{87}Rb in nitrate and halide molten salts, spin-lattice relaxation times are apparently dominated by quadrupolar cou-

pling.[38,200-202] Electric field gradients were estimated from models of the relaxation process, and models of diffusion were explored. Correlation times suggested that the nitrate anion persists for times orders of magnitude longer than the minimum required by vibrational spectra even at 600 °C.

T_1 results for quadrupolar nuclei in molten alkali nitrates and halides have several features in common with a number of other systems, including some of the glasses and ionic conductors described above, and some of the liquid metals described below. Both activation energies and calculated correlation times are often considerably smaller than those determined for long-range diffusion. In nitrates, this observation was originally attributed to association of Na^+ with rotating nitrate grups.[38] Later work pointed out the similar behavior of nonmolecular halide and metal systems, and showed that as in those materials, small local structural fluctuations can cause large changes in electric field gradients and thus dominate relaxation.[201,202] Neither strongly correlated motions nor complete jumps to new sites are required.

As in many other materials described here, application of pulsed field gradient methods to molten salts such as $NaNO_3$ have given accurate, direct measurements of diffusivity at high temperature.[47]

IX. The Transition from Molten Salt to Liquid Metal

The mutual solubility of liquid alkali metals and alkali halides provides an intriguing opportunity to study the transition in structure, bonding, and mechanism of electrical conduction from the electronic to the ionic. The compositional transition from metal to nonmetal generally causes decreases in electronic conductivity by factors of up to 10 000.[203] High-temperature NMR studies have been made of a number of these systems, including Cs–CsI,[204-206] Cs–CsCl,[205] Na–NaBr,[203,205,207] and Na–NaI.[203] The first of these has a remarkable range of stable liquids at temperatures above about 700 °C, ranging from pure liquid Cs metal through the molten salt CsI toward the molecular liquid I_2. ^{133}Cs and ^{127}I NMR studies of both resonance shifts and relaxation showed that when excess metal is initially added to CsI, electrons are strongly localized in F center-like sites.[205] Addition of more Cs rapidly increases electron mobility, with the transition to metallic conductivity at 5–20% excess Cs. The nonlinearity of this change, and comparable results for Cs–CsCl, are shown in Figure 13. Adding excess I to CsI also produced paramagnetic centers, presumed to be the molecular species I_2^-. In contrast to the Cs–CsI system, electrical conductivity in Na–NaBr liquids increases less than linearly with the addition of metal to the molten salt. NMR data showed that electron mobility was independent of added metal concentration out to 5% excess Cs (Figure 13), resulting in a linear relation between relaxation time and composition and supporting a model of spin pairing to form Na_2 dimers.[203,205] This effect may well be related to clustering and the phase separation that is observed in this system.[205] ^{209}Bi NMR on Bi–$BiBr_3$ and Bi–BiI_3 melts showed quite different local dynamics for the two systems, with evidence for clustering or "molecule" formation only in the former system.[208-209]

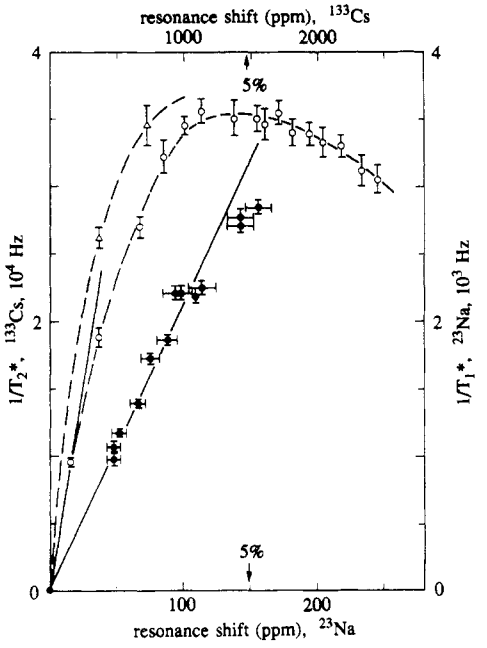

Figure 13. Relaxation rates for ^{133}Cs in Cs–CsI (open circles, 640 °C) and Cs–CsCl (open triangles, 650 °C) and ^{23}Na in Na–NaBr (solid circles, 780 °C) liquids plotted against the relative shift in peak position, which varies systematically with composition. ^{23}Na $1/T_1$ results are referenced to the right-hand and lower scales; inverse line widths for ^{133}Cs (equivalent to $1/T_1$ in these samples) are referenced to the left-hand and upper scales. Arrows labeled "5%" show shifts for the liquids containing 5 mole % metal added to the molten salts (reprinted from ref 205; copyright 1983 American Physical Society).

The electronic properties of certain liquid metal alloys resemble those of true ionic liquids near to the stoichiometries of intermetallic compounds. These materials (e.g. CsAu) are described below in section X.B.

X. Metals and Semimetals

NMR has long been used to study the physics and chemistry of both solid and liquid metals,[205,210-217] including a few studies where solid–liquid phase relations were directly observed.[217] Experiments and theory often combine information on pure metals and alloys, and on compositions ranging from nonmetals to good conductors. Nonetheless, some somewhat arbitrary distinctions between studies emphasizing different aspects of these continua will be made here for clarity. Recently, techniques other than conventional NMR have been developed that extend measurements of Knight shifts and nuclear quadrupolar relaxation to a much larger group of isotopes and to very dilute concentration ranges. These kinds of studies will be mentioned only briefly, but they have been particularly useful in understanding the structure and dynamics of liquid metals at high temperature. As recently reviewed,[214,218,219] and as mentioned above for β radiation detected NMR, these methods are based on the formation of short-lived radioisotopes (with nuclear quadrupolar moments) during bombardment of a sample with a particle beam. In "time-dependent perturbed angular distribution" (TDPAD) experiments, the isomers are usually generated by a pulsed α particle beam. The decay in the initially anisotropic γ radiation that is emitted is then monitored as a function of time, and the spin–lattice relaxation rate is obtained.

A. Single Component Systems: Electronic Structure

High-temperature studies of pure metals have often been concerned with the physics of electronic conduction and magnetic susceptibility and will be discussed only briefly. A good example of this type of study is that of pure crystalline Pt,[220] where Knight shift and T_1 data up to about 1100 °C were quantitatively interpreted in terms of models of electronic structure. Early studies of a variety of relatively low melting point metals noted the surprisingly small effects of melting in a number of systems.[210] In studies of solid and liquid Cu and Al,[211,221] the behaviors of monovalent and polyvalent metals were contrasted. For the former, the temperature-induced change in the Knight shift is dominated by bulk thermal expansion, and the loss of order on melting has little effect. For Al, structural changes are more significant. NMR measurements on pure Mn explored the effects of both crystalline phase transitions and melting.[23]

In contrast to metals with high conductivity, chemical shift anisotropy and atomic diffusion are important influences on relaxation of the dipolar nucleus ^{77}Se in the pure semimetal selenium.[222] Very recent work on single crystals of Se to its melting point of 217 °C, and of Te to about 400 °C, used site selective excitation to measure slow exchange among magnetically inequivalent sites.[162] This technique has considerable promise for studying diffusion mechanisms in noncubic metals and other materials.

Liquid Se at pressures and temperatures into the supercritical fluid range was studied in what must be one of the most "heroic" NMR experiments ever conducted.[12] Measurements to 1625 °C and 790 bars (on explosive, extremely toxic, extremely expensive isotopicly enriched samples) determined the abundance and mobility of paramagnetic centers from the solid and liquid polymeric semiconductor phases, to the low density molecular insulator Se_2 vapor, to the high-pressure metallic liquid. Molecular mobility, concentrations of broken chains and rates of chain breaking, and the electronic bases of the semiconductor to insulator and semiconductor to metal transitions were all quantified.

The reduction in electron density caused by heating toward the liquid–gas critical point can have major effects on the Knight shift and relaxation in alkali metals also, as shown in other technically difficult high-pressure and high-temperature NMR experiments to 1590 °C and pressures to 900 bars on Cs.[223-226] The level of detail on electronic structure provided by these studies has been of major importance in the theoretical understanding of simple liquid metals.[216]

B. Electronic Structure of Liquid Alloys

Liquid alloys have also been studied by NMR to elucidate transitions in electronic structure and mobility. Early work has been reviewed,[217] and the common effects of electron localization were noted. If clustering, or unlike atom pairing or bonding occurs, reduced conduction electron mobility may affect both the Knight shift and the electron-induced relaxation rate, and correlate with large reductions in conductivity.

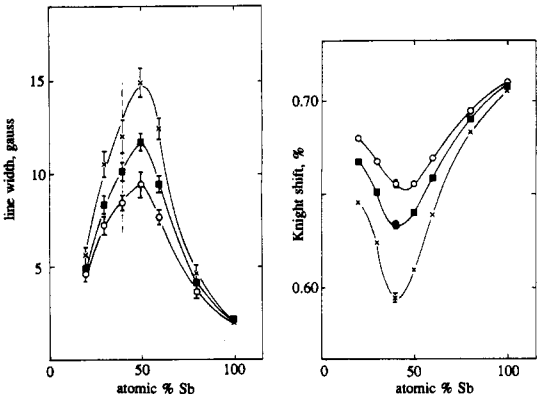

Figure 14. ^{121}Sb NMR data for liquids in the Sb–Te system, illustrating nonlinear effects due to clustering. ×'s are data at 623 °C; squares at 723 °C; circles at 823 °C. Part a shows line width vs concentration of Sb (dashed line shows the composition Sb_2Te_3). Part b shows Knight shift (reprinted from ref 229; copyright 1984 Zeitschrift für Naturforschungen).

These effects were noted, for example, for ^{77}Se and ^{125}Te (both dipolar nuclei) in the liquid semiconductor Se-Te.[227] Minima in Knight shifts and maxima in line widths (due to increased relaxation rates) near to stoichiometric compositions suggested clustering in Bi–Te[228] and in Sb–Te melts.[229,230] Results for the latter are shown in Figure 14. Here the typical effects of temperature can be noted: at higher temperature, disorder increases, clustering decreases, and the nonlinearities of the compositional control on Knight shift and relaxation rate are reduced. Similar conclusions for Tl–Te liquids were based on TDPAD measurements.[231] Liquid Li–Pb and Li–Sn alloys also display both T_1 and Knight shift anomalies near to fixed stoichiometries,[232] and data for Li–Si liquids suggest clustering as well.[233] In–Ga liquids have also been investigated in several studies.[234] As Sb is added to liquid Cs or Na, electrical conductivity, Knight shifts, and relaxation rates are all reduced to nonmetallic values near to the 1:3 compositions,[235-237] again suggesting the presence of relatively long-lived atom clusters. In the Cs–Au binary, the liquid at the 1:1 stoichiometry behaves more like a molten salt as CsI than a liquid metal. Several ^{133}Cs NMR studies indeed indicated a strong localization of electrons on melting of the CsAu compound.[4,238,239] Recently, a thermodynamically based model of atom association (related to that described below for quadrupolar relaxation) has had some success in quantifying the relationship between bonding and Knight shift in liquid semiconductors.[240,241] The combined effects of association and paramagnetic transition-metal atoms on Knight shifts have recently been investigated in the Bi–In–Ni system.[242]

C. Electronic Structure of Solid Intermetallic and Intercalation Compounds

A number of intermetallic superconducting alloys have been studied by NMR at high as well as low temperatures. For example, V_3Si, V_3Au, V_3Co, and V_3Pt are all ordered "A-15" or β-tungsten phases. ^{51}V T_1 measurements up to about 1100 °C were used to constrain models of electronic structure and interactions.[243-246] A correlation between the superconducting critical temperature and the temperature coefficient of the Knight shift was found. More recently, a study by

^{9}Be NMR at high temperature of UBe_{13} was made.[247]

A variety of ordered phases can be made with alkali metals intercalated in graphite. In RbC_8, for example, a first-order transition to a disordered structure at 302 °C was observed by both ^{13}C and ^{87}Rb NMR.[248] Disordering and diffusion in CsC_{24} has been studied by ^{133}Cs NMR up to about 350 °C.[249]

D. Atomic Structure and Dynamics in Liquid Metals

A second type of NMR study of metals has more in common with those on other materials described in this review: the determination of rates and mechanisms of atomic diffusion in both solids and liquids and implications for structure and atom association or bonding. As in the silicates, ionic conductor solids, and molten salts described above, relaxation time data can provide important constraints on diffusion, but need to be interpreted with care in order to distinguish among multiple relaxation mechanisms and multiple time and length scales for dynamics. From the earliest relaxation studies of liquid metals onward, discrepancies between observations and results expected for simple models of diffusion and motion were noted.[250-253] As in other systems, pulsed field gradient NMR techniques have yielded more direct measurements of diffusivity in liquid metals such as Li,[254-256] but are often difficult to apply because of very short relaxation times common in metallic systems.

In good conductors such as alkali metals, Cu, and Al, as well as in some liquid alloys such as In–Zn,[257] NMR spin–lattice relaxation times are generally dominated by magnetic interactions with the conduction electrons and do not provide a great deal of structural information about atomic structure.[207] However, in many metals with lower conductivities, and/or large electric field gradients that can interact with nuclear spins, a quadrupolar component to the relaxation can be separated out. When a pair of isotopes exists with different Larmor frequencies and quadrupolar couplings, this calculation can be especially accurate. Subtraction of the magnetic component calculated from the Korringa relation is also possible, but is more dependent on theory. Theories of quadrupolar relaxation consider local interactions, including three-body terms,[258,259] and thus can give structurally interesting results. These models successfully explained the common observation that $1/T_1$ in these systems if often approximately proportional to $T^{-1/2}$, not to T^{-1} as expected from simple BPP theory. As in nonmetallic systems, the common finding that the activation energy for T_1 for quadrupolar nuclei in liquid metals is considerably less than that for tracer diffusion results from the large effects of small, local, atomic motions, which can cause large fluctuations in the electric field gradient.[258,259] More recent theory based on mode coupling again noted the fast relaxation caused by rapid fluctuations around local equilibrium positions.[260]

In liquid alloys, the quadrupolar relaxation rate is often substantially increased from those of the pure constituents, in contrast to the decreases in the contribution from conduction electrons noted above. In relatively weakly interacting systems, theories of local fluctuations in the density of like and unlike neighbor atoms have been developed, and applied to NMR and TDPAD data for a wide variety of alloys.[261-264] Because "nuclear" methods largely fall outside of the scope of this review, results from the latter technique will be mentioned only briefly. Systems with stronger interactions are often characterized by high melting point (i.e. highly stable) intermediate compounds, as well as increases in viscosity, decreases in conductivity, and large negative heats of mixing at intermediate compositions. Quadrupolar relaxation rates in these systems can be increased by as much as three orders of magnitude from those of the pure liquids. Numerous studies were reviewed in detail very recently[265] and are described in a long series of earlier experimental and theoretical papers.[261,266-273] It was found that in binary and ternary alloys with the strongest interactions quadrupolar relaxation rates were increased most. Increasing temperature was found to generally decrease the rate, and this effect was greatest in compositions where the largest alloying effect was noted. Apparently, relatively long-lived associations or unlike atom pairs result in slower fluctuations in the local field gradient, enhancing the relaxation process. Increasing temperature increases disorder, and decreases the lifetimes and number density of pairs. These findings led to a detailed thermodynamic or "quasi-chemical" theory of atom association and its effects on relaxation and Knight shifts. Although not capable of treating all details of the experimental observations, the good correlations obtained between nuclear spin physics and chemical models is impressive. In some cases, the changes with composition in the relaxation rate predicted from interaction energies (based only on thermodynamic data) are within 10–20% of those observed.[260]

A number of high-temperature β-detected NMR studies, primarily of ^{8}Li in Li liquid alloys, have been made.[219,274,275] In systems with strong unlike atom association, increased electron localization was again detected by the reduction in the electronic contribution to relaxation and the Knight shift.

E. Defects and Trace Impurities in Solid Metals

The intensity of the NMR line for a quadrupolar nuclide in a pure solid can be greatly reduced by small concentrations of impurities, because of increases in electric field gradients that can be significant out to several coordination spheres around an impurity atom.[35] This effect may be reduced by motional averaging as temperature increases and was exploited to study diffusional dynamics in dilute Al–Zn alloys.[276]

Impurities can also greatly influence spin–lattice relaxation, if they are mobile within a structure. In a study of solid Al containing 0.02 to about 1% of Ti, Cr, Mn, or Cu, it was shown that relative diffusional jumping of solute and Al atoms could be quantified.[277] A series of NMR studies of relaxation, Knight shifts, and line widths in niobium and vanadium have shown that spin–lattice relaxation follows the normal Korringa relation (the product of T_1 and temperature is approximately constant), except for a peak in relaxation rate near 700 °C caused by an increased mobility of oxygen and other impurities.[23,278-280] Rates of impurity and self diffusion were calculated. The more recent study also included measurements of the rotating frame relaxation time $T_{1\rho}$ to the extremely high temperature

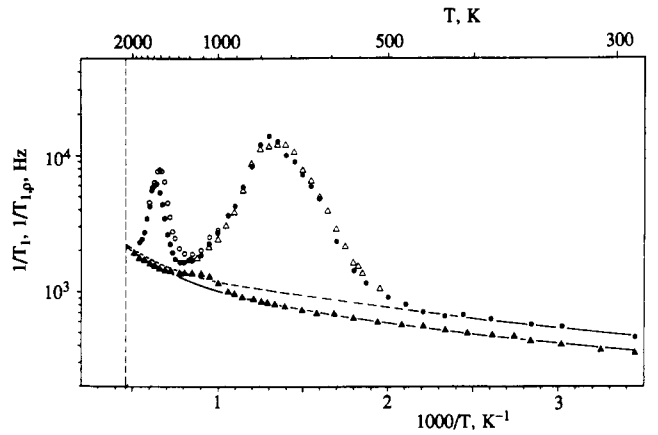

Figure 15. $1/T_1$ (solid triangles) and $1/T_{1\rho}$ (other symbols) for ^{51}V in polycrystalline vanadium metal, plotted against inverse temperature. Dashed line shows melting point (reprinted from ref 24; copyright 1983 Pergamon Press).

of 1700 °C.[23] Because $T_{1\rho}$ is controlled by much slower motions than T_1, the former is often much more sensitive to diffusive motion in solids. As shown by Figure 15, two peaks in $1/T_{1\rho}$ were observed. At lower temperature, the effect previously noted of oxygen motion is apparent and was confirmed by the increase in the relaxation rate with time as this contaminant diffused into the sample. At higher temperature, a second peak in $1/T_{1\rho}$ was attributed to the motion of the V atoms themselves. Diffusion rates and mechanisms for both species were determined and correlated with tracer diffusivity.

The creep of dislocations caused by plastic deformation can substantially enhance quadrupolar relaxation, as described for salts in a previous section. This approach has been applied to Al metal and shows promise for important new insights into deformation mechanisms in metals at low as well as high temperatures.[171]

F. Hydrogen in Solid Metals, Semimetals, and Hydrides

Hydrogen in a variety of metals and semimetals has been studied by NMR. Work at high temperatures has included the diffusion of H in amorphous Si films to about 500 °C[273] and dynamical studies of several scandium hydrides.[282] In the latter materials, ^{45}Sc T_1 data showed a second high temperature minimum (Figure 16), indicating a second mode of H motion with a relatively long correlation time for Sc–H interactions. This anomalous behavior, as well as results from ^1H and ^2H NMR,[283] was explained by increased repulsions at energetic saddle points in the diffusion path caused by increased vibrational anharmonicity, which theoretically can reduce H mobility at higher temperature.[284] However, further studies of materials with relatively dilute hydrogen, such as $VH_{0.2}$ and $NbH_{0.2}$,[285] as well as neutron scattering and pulsed field gradient measurements to 1000 °C, made this model untenable.[286] Hydrogen clustering or other correlated motion has been proposed as an explanation of the anomalous double T_1 minima,[286,287] and the intriguing similarity to the behavior of PbF_2 (isostructural with ScH_2) was noted (section V and ref 104).

The diffusion constant for H has been measured directly by the pulsed field gradient technique in TiH_x

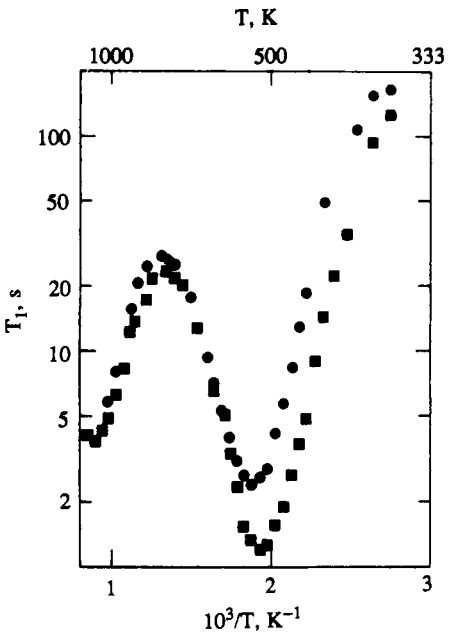

Figure 16. The effect of temperature on T_1 for ^{45}Sc in $ScH_{1.83}$. Solid circles represent data collected at 24 MHz; solid squares, 12.2 MHz. Note the presence of a second minimum at high temperature (reprinted from ref 282; copyright 1987 American Physical Society).

to 550 °C.[288] The finding of well-defined T_1 minima allowed an accurate determination of the correlation time for diffusive site hopping, and a combination of the two types of data gave an unusually well-constrained model of the jump distance and diffusion mechanism. Similar results were obtained for $NbH_{0.6}$.[289]

XI. Prospects for Future Work

Spectroscopy done in situ at extremes of temperature or pressure is not likely to be "routine". However, some applications of high-temperature NMR, such as relaxation time studies of liquid metals and solid ionic conductors, certainly have become relatively common, well-established parts of the experimental repertoire. Several factors are driving the field in new directions.

The most obvious of these is the development of new experimental technology. In particular, the spectrometers and high-field magnets originally developed to increase sensitivity and resolution in spectroscopy of complex organic molecules are being used more and more for studies of inorganic solids and liquids. Some of this work has now been extended to very high temperatures. Because signal strength from a given sample at a given temperature generally increases dramatically with increased magnetic field, experiments on a greater variety of nuclei in solids have become feasible. Some of those mentioned here include ^{17}O,[89,115,116,177] ^{29}Si,[6,32,79,86-88] ^{39}K,[174] and ^{47}Ti.[81,162,166,167] Studies of ^{13}C spectra in static solids and viscous liquids at high temperature and pressure are also in this category of "newly accessible nuclei".[69,248]

In many studies at relatively low field on abundant isotopes with high Larmor frequencies (e.g. ^1H, ^7Li, ^{19}F, ^{23}Na, and ^{27}Al), line shapes in solids are dominated by dipolar broadening. Line widths, and narrowing with increased temperature, can give some structural and dynamical information, but this is often limited to average interatomic distances and jump frequencies.

Recent work at fields as high as 8–12 T has shown that in some cases, static quadrupole or chemical shift powder patterns become resolvable, which can provide greater structural detail.[18,19] MAS[41,43–45,69,70,72,73,75,76,178] and multipulse line narrowing techniques[113] are also beginning to be applied at high temperature to further improve resolution. Information on site exchange becomes correspondingly more specific when inequivalent sites can be distinguished in spectra.

In one sense, relaxation time studies at high magnetic fields have been hindered by the very technology that makes them possible: superconducting NMR magnets are generally set up to operate at only a single field strength. This makes the determination of frequency dependence (crucial in the understanding of relaxation mechanisms) more difficult than with lower field electromagnets. The development of superconducting NMR magnets with relatively easily adjustable fields, or, more likely, the eventual access to greater numbers of instruments with different fixed fields, should resolve this difficulty.

Relatively new types of NMR experiments are also beginning to be applied to the study of materials at high temperature, as access to modern spectrometers increases. Methods that can observe very slow dynamics, such as 2-D exchange and nutation spectroscopy[18,19,78,90,172] and site-selective excitation,[162] are particularly interesting. Multinuclear experiments that can directly measure couplings (and therefore distances and exchange dynamics) among different nuclei may prove to be very important.

The technology of three-dimensional NMR microimaging does not yet seem to have been applied at high temperature, but clearly offers a wealth of possibilities. The most obvious of these include the in situ observation of melting in a multiphase solid, and the changes in pore volume and shape that occur during reactions with gases or liquids. These problems are of particular interest in ceramics science and in geophysics.

Several elegant new applications of high-temperature technology (c.f. section I) have recently made new types of high-temperature NMR possible. These include containerless, laser-heated techniques[1,84,85,172] and sophisticated control of gas-phase composition.[81,167] Developments such as these are greatly improving the prospects for new measurements on oxides and silicates at extreme temperatures. Better atomic-scale understanding of both solids and liquids important in materials and the earth sciences should follow.

Acknowledgments. I thank my many colleagues who sent preprints and reprints of recent high-temperature NMR studies. This work was supported in part by grants from the National Science Foundation, Nos. NSF EAR 85-53024 and EAR 89-05188, to J.F.S.

References

(1) Taulelle, F.; Coutures, J. P.; Massiot, D.; Rifflet, J. P. *Bull. Magn. Reson.* **1989**, *11*, 318.
(2) Bloembergen, N.; Purcell, E. M.; Pound, R. V. *Phys. Rev.* **1948**, *73*, 679.
(3) Warren, W. W. In *Molten Salt Techniques*; Lovering, D. G.; Gale, R. J., Eds.; Plenum Press: New York, Vol. 4, in press.
(4) Dupree, R.; Kirby, D. J.; Warren, W. W., Jr. *Phys. Rev. B* **1985**, *31*, 5597.
(5) Roe, D. C. *J. Magn. Reson.* **1985**, *63*, 388.
(6) Stebbins, J. F.; Schneider, E.; Murdoch, J. B.; Pines, A.; Carmichael, I. S. E. *Rev. Sci. Instr.* **1986**, *57*, 39.
(7) Ploumbidis, D. *Appl. Spectr.* **1982**, *3*, 314.
(8) Horvath, I. *Chem. Rev.* **1991**, *91*, this issue.
(9) Shimokawa, S.; Yamada, E.; Makino, K. *Bull. Chem. Soc. Jpn.* **1983**, *56*, 412.
(10) DeFries, T. H.; Jonas, J. *J. Magn. Reson.* **1979**, *35*, 111.
(11) Shimokawa, S.; Yamada, E. *J. Magn. Reson.* **1983**, *51*, 103.
(12) Warren, W. W., Jr. *Phys. Rev. B* **1980**, *22*, 2257.
(13) Griffiths, T. R. In *Molten Salt Techniques*; Gale, R. J.; Lovering, D. G., Eds.; Plenum Press, New York, 1983; Vol. 2, p 79.
(14) Jäger, C.; Scheler, G. *Expt. Tech. Phys.* **1984**, *32*, 315.
(15) Aurora, T. S.; Day, S. M. *Rev. Sci. Instr.* **1982**, *53*, 1152.
(16) Ploumbidis, D. *Rev. Sci. Instr.* **1979**, *50*, 1133.
(17) Clark, L. D. *Rev. Sci. Instr.* **1969**, *40*, 1498.
(18) Janssen, R.; Tijink, G. A. H.; Veeman, W. S.; Maesen, Th. L. M.; Van Lent, J. F. *J. Phys. Chem.* **1989**, *93*, 899.
(19) Janssen, R. Investigation of Zeolites by Solid State Quadrupole NMR. Thesis, University of Nijmegen, The Netherlands, 1990.
(20) Schreiber, D. S. *Rev. Sci. Instr.* **1964**, *35*, 1582.
(21) Doty, D. *Abstracts*, Rocky Mountain Conference in Analytical Chemistry; American Chemical Society: Washington, DC, 1990; p 32.
(22) Hafner, S.; Nachtrieb, N. H. *Rev. Sci. Instr.* **1964**, *35*, 680.
(23) El-Hanany, U.; Warren, W. W., Jr. *Phys. Rev. B* **1975**, *12*, 861.
(24) Günther, B.; Kanert, O. *Acta Metall.* **1983**, *31*, 909.
(25) Shaham, M.; El-Hanany, U. *J. Phys. E: Sci. Instr.* **1979**, *12*, 359.
(26) Warren, W. W., Jr.; Clark, W. G. *J. Sci. Instr., Ser. 2* **1968**, *1*, 1019.
(27) Webster, D. S.; Cross, L. F.; Lynch, L. J. *Rev. Sci. Instr.* **1979**, *50*, 390.
(28) Soller, F. X.; Sotier, S.; Coufal, H.; Hackstein, K. *J. Phys. E: Sci. Instr.* **1979**, *12*, 577.
(29) Styles, G. A.; Sheffield, T. B. *J. Phys. E: Sci. Instr.* **1976**, *9*, 223.
(30) Ploumbidis, D. *Expt. Tech. Phys.* **1982**, *30*, 323.
(31) Kolem, H.; Kanert, O.; Schulz, H. *J. Magn. Reson.* **1990**, *87*, 160.
(32) Shimokawa, S.; Maekawa, H.; Yamada, E.; Maekawa, T.; Nakamura, Y.; Yokokawa, T. *Chem. Lett.* **1990**, 617.
(33) Haddix, G. W.; Reimer, J. A.; Bell, A. T. *J. Catal.* **1987**, *106*, 111.
(34) Davis, M. E.; Hathaway, P.; Morgan, D.; Glass, T.; Dorn, H. In *Catalysis 1987*; Ward, J. W., Ed.; Elsevier: Amsterdam, 1988; p 263.
(35) Abragam, A. *Principles of Nuclear Magnetism*; Clarendon Press: London, 1961.
(36) Hoult, D. I.; Richards, R. E. *J. Magn. Reson.* **1976**, *24*, 71.
(37) Hill, H. D. W.; Richards, R. E. *J. Sci. Instr., Ser. 2* **1968**, *1*, 977.
(38) Harold-Smith, D. *J. Chem. Phys.* **1973**, *59*, 4771.
(39) Adler, S. B.; Micheals, J. N.; Reimer, J. A. *Rev. Sci. Instr.* **1990**, *61*, 3368.
(40) Maresch, G. G.; Kendrick, R. D.; Yannoni, C. S. *Rev. Sci. Instr.* **1990**, *61*, 77.
(41) Crosby, R. C.; Haw, J. F.; Lewis, D. H. *Anal. Chem.* **1988**, *60*, 2695.
(42) Gieschke, D.; Quillfeldt, E. *J. Magn. Reson.* **1985**, *65*, 326.
(43) Stebbins, J. F.; Farnan, I.; Williams, E.; Roux, J. *Phys. Chem. Miner.* **1989**, *16*, 763.
(44) Haw, J. F. *Anal. Chem.* **1988**, *60*, 559A.
(45) Haw, J. F.; Campbell, G. C.; Crosby, R. C. *Anal. Chem.* **1986**, *58*, 3172.
(46) Gordon, R. E.; Strange, J. H.; Webber, J. B. W. *J. Phys. E: Sci. Instr.* **1978**, *11*, 1051.
(47) Herdlicka, C.; Richter, J.; Zeidler, M. D. *Z. Naturforsch.* **1988**, *43a*, 1075.
(48) Akasaka, K.; Naito, A.; Nakatani, H.; Imanari, M. *Rev. Sci. Instr.* **1990**, *61*, 66.
(49) Shimokawa, S. E.; Yamada, E. *Rev. Sci. Instr.* **1985**, *56*, 1220.
(50) English, A. D.; Garza, O. T. *Macromolecules* **1979**, *12*, 351.
(51) Sterna, L. L.; Smith, H. C. *J. Magn. Reson.* **1988**, *79*, 528.
(52) English, A. D.; Vega, A. J. *Macromolecules* **1979**, *12*, 353.
(53) Wilson, M. A. *NMR Techniques and Applications in Geochemistry and Soil Chemistry*; Pergamon: New York, 1987.
(54) Lynch, L. J.; Webster, D. S.; Bacon, N. A.; Barton, W. A. In *Magnetic Resonance. Introduction, Advanced Topics and Applications to Fossil Energy*; Petrakis, L.; Fraissard, J. P., Eds.; E. Reidel: Dordrecht, 1984; p 617.
(55) Lynch, L. J.; Webster, D. S. *Fuel* **1982**, *61*, 271.
(56) Yokono, T.; Miyazawa, K.; Sanada, Y.; Marsh, H. *Fuel* **1981**, *60*, 603.
(57) Miyazawa, K.; Yokono, T.; Sanada, Y. *Carbon* **1979**, *17*, 223.
(58) Webster, D. S.; Lynch, L. J. *Fuel* **1981**, *60*, 549.
(59) Lynch, L. J.; Webster, D. S.; Sakurovs, R.; Barton, W. A.; Maher, T. P. In *Proceedings, 1985 International Conference on Coal Science*; Pergamon Press: New York, 1985; p 887.

(60) Yokono, T.; Iyama, S.; Sanada, Y.; Shimokawa, S.; Yamada, E. *Fuel* **1986**, *65*, 1701.
(61) Yokono, T.; Iyama, S.; Sanada, Y.; Makino, K. *Fuel* **1985**, *64*, 1014.
(62) Yokono, T.; Iyama, S.; Sanada, Y.; Shimokawa, S.; Yamada, E. In *Proceedings, 1985 International Conference on Coal Science*; Pergamon Press: New York, 1985; p 766.
(63) Harrell, J. W., Jr.; Kohno, T. In *Magnetic Resonance. Introduction, Advanced Topics and Applications to Fossil Energy*; Petrakis, L.; Fraissard, J. P., Eds.; E. Reidel: Dordrecht, 1984; p 597.
(64) Singer, L. S. *Fuel* **1981**, *60*, 839.
(65) De Lopez, H.; Yokono, T.; Takahashi, N.; Sanada, Y. *Fuel* **1988**, *67*, 301.
(66) Miyakawa, K.; Yokono, T.; Sanada, Y.; Yamada, E.; Shimokawa, S. *Carbon* **1981**, *19*, 143.
(67) Shimokawa, S.; Yamada, E.; Yokono, T.; Iyama, S.; Sanada, Y. *Carbon* **1984**, *22*, 433.
(68) Azami, K.; Yokono, T.; Sanada, Y.; Uemura, S. *Carbon* **1989**, *27*, 177.
(69) Yokono, T.; Takahashi, N.; Kaneko, T.; Sanada, Y. *Fuel* **1990**, *69*, 796.
(70) Haw, J. F.; Richardson, B. R.; Lazo, N. D.; White, J.; Schettler, P. *Experimental NMR Conference* **1989**, *30*, 97.
(71) Pruski, M.; Kelzenberg, J. C.; King, T. S.; Gerstein, B. C. *Experimental NMR Conference* **1989**, *30*, 97.
(72) Lazo, N. D.; White, J. L.; Munson, E. J.; Lambregts, M.; Haw, J. F. *J. Am. Chem. Soc.* **1990**, *112*, 4050.
(73) White, J. L.; Lazo, N. D.; Richardson, B. R.; Haw, J. F. *Catal.* **1990**, *125*, 260.
(74) Schöllinger, R.; Herden, H. J. In *Molecular Sieves – II*; Katzer, J. R., Eds.; American Chemical Society: Washington, DC, 1977; p 357.
(75) Strobl, H.; Fyfe, C. A.; Kokotailo, G. T.; Pasztor, C. T. *J. Am. Chem. Soc.* **1987**, *109*, 4733.
(76) Fyfe, C. A.; Kokotailo, G. T.; Strobl, H.; Gies, H.; Kennedy, G. J.; Pasztor, C. T.; Barlow, G. E. In *Zeolites as Catalysts*; Karge, H. G.; Weitkamp, J., Eds.; Elsevier: Amsterdam, 1989, p 827.
(77) Kanert, O. *Cryst. Lattice Defects Amorphous Mater.* **1985**, *12*, 41.
(78) Janssen, R.; Dols, P. P. M. A.; Tijink, G. A. H.; Veeman, W. S. In *Zeolites: Facts, Figures, Futures*; Jacobs, P. A.; Van Santen, R. A., Eds.; Elsevier: Amsterdam, 1989; p 609.
(79) Farnan, I.; Stebbins, J. F. *J. Am. Chem. Soc.* **1990**, *112*, 32.
(80) Shannon, R. D.; Taylor, B. E.; English, A. D.; Berzins, T. *Electrochim. Acta* **1977**, *22*, 783.
(81) Kanert, O.; Kolem, H. *J. Phys. C: Solid State Phys.* **1988**, *21*, 3909.
(82) Stebbins, J. F.; Farnan, I.; Klabunde, U. *J. Am. Ceram. Soc.* **1989**, *72*, 2198.
(83) Davis, M. E.; Murray, B. D.; Narayana, M. In *Novel Materials in Heterogeneous Catalysis*; Baker, R. T. K.; Murrell, L. L., Eds.; American Chemical Society: Washington, DC, 1990; p 48.
(84) Coutures, J. P.; Massiot, D.; Bessada, C.; Echegut, P.; Rifflet, J. C.; Taulelle, F. *C.R. Acad. Sci., Ser. 2* **1990**, *310*, 1041.
(85) Massiot, D.; Taulelle, F.; Coutures, J. P. *J. Phys., Colloq.* **1990**, *51*, C5-425.
(86) Liu, S. B.; Stebbins, J. F.; Schneider, E.; Pines, A. *Geochim. Cosmochim. Acta* **1988**, *52*, 527.
(87) Stebbins, J. F. *J. Non-Cryst. Solids* **1988**, *106*, 359.
(88) Liu, S. B.; Pines, A.; Brandriss, M.; Stebbins, J. F. *Phys. Chem. Miner.* **1987**, *15*, 155.
(89) Farnan, I.; Stebbins, J. F. *Experimental NMR Conference* **1990**, *31*, 153.
(90) Farnan, I.; Stebbins, J. F. *J. Non-Cryst. Solids* **1990**, *124*, 207.
(91) Rubenstein, M.; Resing, H. A. *Phys. Rev. B* **1976**, *13*, 959.
(92) Rubenstein, M.; Resing, H. A.; Reinecke, T. L.; Ngai, K. L. *Phys. Rev. Lett.* **1975**, *34*, 1444.
(93) Berthier, C. In *Fast Ionic Transport in Solids*; Vashishta, P.; Mundy, J. N.; Shenoy, G. K. Eds.; North-Holland: Amsterdam, 1979; p 171.
(94) Chandra, S. *Superionic Solids*; North-Holland: Amsterdam, 1981.
(95) Whittingham, M.; Silbernagel, B. G. In *Solid Electrolytes*; Hagenmuller, P.; Van Gool, W. Eds.; Academic Press: New York, 1978; p 93.
(96) Story, H. S.; Bailey, W. C.; Chung, I.; Roth, W. L. In *Superionic Conductors*; Mahan, G. D.; Roth, W. L., Eds.; Plenum Press: New York, 1976, p 317.
(97) Richards, P. M. In *Physics of Superionic Conductors*; Salamon, M. B., Ed.; Springer-Verlag: Berlin, 1979; p 141.
(98) Martin, S. W. *Mater. Chem. Phys.* **1989**, *23*, 225.
(99) Bjorkstam, J. L.; Listerud, J.; Villa, M. *Solid State Ionics* **1986**, *18/19*, 117.
(100) Eisenstadt, M. *Phys. Rev.* **1963**, *132*, 630.
(101) Lysiak, R. J.; Mahendroo, P. P. *J. Chem. Phys.* **1966**, *44*, 4025.
(102) Gordon, R. E.; Strange, J. H. *J. Phys., Colloq.* **1976**, *C7*, 476.
(103) Gordon, R. E.; Strange, J. H. *J. Phys. C: Solid State Phys.* **1978**, *11*, 3213.
(104) Boyce, J. B.; Mikkelsen, J. C., Jr.; O'Keefe, M. *Solid State Commun.* **1977**, *21*, 955.
(105) Cassanho, A.; Guggenheim, H.; Walstedt, R. E. *Phys. Rev. B* **1983**, *27*, 6587.
(106) Chadwick, A. V.; Hope, D. S.; Joroszkiewicz, G.; Strange, J. H. In *Fast Ionic Transport in Solids*; Vashishta, P.; Mundy, J. N.; Shenoy, G. K. Eds.; North-Holland: Amsterdam, 1979; p 683.
(107) Livshits, A. I.; Buznik, V. M.; Fedorov, P. P.; Sobolev, B. P. *Inorg. Mater.* **1982**, *18*, 114.
(108) Aalders, A. F.; Polman, A.; Arts, A. F. M.; De Wijn, H. W. *Solid State Ionics* **1983**, *9/10*, 539.
(109) Roos, A.; Aalders, A. F.; Schoonman, J.; Arts, A. F. M.; de Wijn, H. W. *Solid State Ionics* **1983**, *9/10*, 571.
(110) Aalders, A. F.; Arts, A. F. M.; De Wijn, H. W. *Solid State Ionics* **1985**, *17*, 241.
(111) Aalders, A. F.; Lochs, H. G. M.; Arts, A. F. M.; De Wijn, H. W. *J. Phys. C: Solid State Phys.* **1986**, 1123.
(112) Aalders, A. F.; Arts, A. F. M.; De Wijn, H. W. *Phys. Rev. B* **1985**, *32*, 5412.
(113) Privalov, A. F.; Vieth, H. M.; Murin, I. V. *J. Phys. Chem. Solids* **1989**, *50*, 395.
(114) Moskvich, Y. N.; Cherkasov, B. I.; Polyakov, A. M.; Sukhovskii, A. A.; Davidovich, R. L. *Phys. State. Sol.* **1989**, *156*, 615.
(115) Fuda, K.; Kishio, K.; Yamauchi, S.; Fueki, K. *J. Phys. Chem. Solids* **1985**, *46*, 1141.
(116) Fuda, K.; Kishio, K.; Yamauchi, S.; Fueki, K.; Onada, Y. *J. Phys. Chem. Solids* **1984**, *45*, 1253.
(117) Chung, I.; Story, H. S. *J. Chem. Phys.* **1975**, *63*, 4903.
(118) Villa, M.; Bjorkstam, J. L. In *Fast Ionic Transport in Solids*; Vashishta, P.; Mundy, J. N.; Shenoy, G. K. Eds.; North-Holland: Amsterdam, 1979; p 289.
(119) Brinkman, D.; Mali, M.; Roos, J.; Story, H. S.; Dubin, R. R. In *Fast Ionic Transport in Solids*; Vashishta, P.; Mundy, J. N.; Shenoy, G. K. Eds.; North-Holland: Amsterdam, 1979; p 285.
(120) Bailey, W. C.; Story, H. S.; Ochadlick, A. R., Jr.; Farrington, G. C. In *Fast Ionic Transport in Solids*; Vashishta, P.; Mundy, J. N.; Shenoy, G. K. Eds.; North-Holland: Amsterdam, 1979; p 281.
(121) Walstedt, R. E.; Dupree, R.; Remeika, J. P.; Rodriguez, A. *Phys. Rev. B* **1977**, *15*, 3442.
(122) Bottyan, L.; Dupree, R.; Chandrashekar, G. V. *Solid State Ionics* **1983**, *9/10*, 347.
(123) Hayes, C. E.; Ailon, D. C. In *Fast Ionic Transport in Solids*; Vashishta, P.; Mundy, J. N.; Shenoy, G. K. Eds.; North-Holland: Amsterdam, 1979; p 297.
(124) Furukawa, Y.; Nakabayashi, Y.; Kawai, S. *Solid State Ionics* **1981**, *3/4*, 85.
(125) Bjorkstam, J. L.; Manzini, S.; Villa, M. In *Fast Ionic Transport in Solids*; Vashishta, P.; Mundy, J. N.; Shenoy, G. K. Eds.; North-Holland: Amsterdam, 1979; p 293.
(126) Li, Z.; Xue, R.; Chen, L. *Chin. Phys.* **1982**, *2*, 933.
(127) Bose, M.; Basu, A.; Torgenson, D. *Solid State Ionics* **1986**, *18/19*, 539.
(128) Petit, D.; Collin, G.; Boilot, J. P. *Mater. Res. Bull.* **1986**, *21*, 365.
(129) Kishio, K.; Owers-Bradley, J. R.; Halperin, W. P.; Brittain, J. O. *Solid State Ionics* **1981**, *5*, 425.
(130) Brinkmann, D.; Mali, M.; Roos, J. In *Fast Ionic Transport in Solids*; Vashishta, P.; Mundy, J. N.; Shenoy, G. K. Eds.; North-Holland: Amsterdam, 1979; p 483.
(131) Brinkman, D.; Freudenreich, W.; Roos, J. *Solid State Commun.* **1978**, *28*, 233.
(132) Messer, R.; Birli, H.; Differt, K. *J. Phys., Colloq.* **1980**, *41*, C6-28.
(133) Kitahama, K.; Furukawa, Y.; Kawai, S.; Nakamura, Y. *Solid State Ionics* **1981**, *3/4*, 335.
(134) Dupree, R.; Howells, J. R.; Hooper, A.; Poulsen, F. W. *Solid State Ionics* **1983**, *9/10*, 131.
(135) Bjorkstam, J. L.; Brinkmann, D.; Mali, M.; Roos, J.; Phipps, J. B.; Skarstad, P. M. *Solid State Ionics* **1986**, *18/19*, 557.
(136) Mali, M.; Roos, J.; Brinkman, D.; Phipps, J. B.; Skarstad, P. M. *Solid State Ionics* **1988**, *28-30*, 1089.
(137) Wang, G.; Li, Z.; Chen, L.; Zhao, Z. *Chin. Phys.* **1982**, *2*, 949.
(138) Follstaedt, D. M.; Richards, P. M. *Phys. Rev. Lett.* **1976**, *37*, 1571.
(139) Schwiekert, E.; Mali, M.; Roos, J.; Brinkman, D.; Richards, P. M.; Biefeld, R. M. *Solid State Ionics* **1983**, *9/10*, 1317.
(140) Wang, G. *Wu Li* **1981**, *10*, 461.
(141) Onoda, Y.; Watanabe, M.; Fujiki, Y.; Yoshikado, S.; Ohachi, T.; Taniguchi, I. *Solid State Ionics* **1981**, *3/4*, 331.
(142) Onoda, Y.; Fujiki, Y.; Yoshikado, S.; Ohachi, T.; Taniguchi, I. *Solid State Ionics* **1983**, *9/10*, 1311.
(143) Onoda, Y.; Watanabe, M.; Fujiki, Y.; Kudo, Y.; Erata, T.; Yoshikado, S.; Ohachi, T.; Taniguchi, I. *Solid State Ionics* **1988**, *28-30*, 179.

(144) Man, P. P.; Theveneau, H.; Papon, P.; Fourquet, J. L. *Solid State Ionics* **1983**, *9/10*, 73.
(145) Boyce, J. B.; Huberman, B. A. *Solid State Commun.* **1977**, *21*, 31.
(146) Kanashiro, T.; Ohno, T.; Satoh, M.; Okamoto, M.; Kojima, A.; Akao, F. *Solid State Ionics* **1981**, *3/4*, 327.
(147) Mousa, M.; Oei, Y. S.; Richtering, H. *J. Phys., Colloq.* **1980**, *41*, C6-223.
(148) Heitjans, P. *Solid State Ionics* **1986**, *18/19*, 50.
(149) Bader, H.; Heitjans, P.; Ackermann, H.; Freiländer, P.; Kiese, G.; Schirmer, A.; Stöckmann, H. J.; Van der Marel, C. *Ann. Phys. (Liepzig)* **1985**, *42*, 169.
(150) Schirmer, A.; Schirmacher, W. *Solid State Ionics* **1988**, *28-30*, 134.
(151) Müller-Warmuth, W.; Eckert, H. *Phys. Rep.* **1982**, *88*, 91.
(152) Göbel, E.; Müller-Warmuth, W.; Olyschläger, H. *J. Magn. Reson.* **1979**, *36*, 371.
(153) Hendrickson, J. R.; Bray, P. J. *J. Chem. Phys.* **1974**, *61*, 2754.
(154) Jain, H.; Balzer-Jöllenbeck, G.; Kanert, O. *J. Am. Ceram. Soc.* **1985**, *68*, C24.
(155) Geissberger, A. E.; Bucholz, F.; Bray, P. J. *J. Non-Cryst. Solids* **1982**, *49*, 117.
(156) Pradel, A.; Ribes, M.; Maurin, M. *Solid State Ionics* **1988**, *28-30*, 762.
(157) Schirmer, A.; Heitjans, P.; Ackermann, H.; Bader, B.; Freiländer, P.; Stöckmann, H. J. *Solid State Ionics* **1988**, *28-30*, 717.
(158) Martin, S. W.; Bischof, M. J.; Mali, M.; Roos, J.; Brinkmann, D. *Solid State Ionics* **1986**, *18/19*, 421.
(159) Roos, J.; Brinkmann, D.; Mali, M.; Pradel, A.; Ribes, M. *Solid State Ionics* **1988**, *28-30*, 710.
(160) Bray, P. J.; Hintenlang, D. E.; Mulkern, R. V.; Greenbaum, S. G.; Tran, D. C.; Drexhage, M. *J. Non-Cryst. Sol.* **1983**, *56*, 27.
(161) De Hossan, J. Th. M.; Kanert, O.; Sleeswyk, A. W. In *Dislocations in Solids*; Nabarro, F.R.N., Ed.; North-Holland: Amsterdam, 1983; p 441.
(162) Kanert, O.; Kolem, H. *Adv. Magn. Reson.* **1989**, *13*, 161.
(163) Richtering, H.; Becker, K. D.; Hamann, H. *J. Phys., Colloq.* **1976**, *37*, C7-373.
(164) Dubiel, M.; Berg, G.; Frölich, F. *Phys. Stat. Sol. B* **1978**, *89*, 595.
(165) Becker, K. D. *J. Phys., Colloq.* **1980**, *41*, C6-249.
(166) Kolem, H.; Kanert, O. *Zeit. Metall.* **1989**, *80*, 227.
(167) Hackman, A.; Kanert, O. *Radiation Effects and Defects in Solids* **1991**, in press.
(168) Alsem, W. H. M.; De Hossan, J. Th. M.; Tamler, H.; Hacklöer, H. J.; Kanert, O. In *Nuclear and Electron Resonance Spectroscopies Applied to Materials Science*; Kaufmann, E. N.; Shenoy, G. K., Eds.; Elsevier North Holland: Amsterdam, 1981; p 481.
(169) De Hossan, J. T. M. In *Dislocations in Solids*; Susuki, H.; Ninomiya, T.; Sumino, K.; Takeuchi, S., Eds.; University of Tokyo Press: Tokyo, 1985, p 261.
(170) Alsem, W. H. M.; Sleeswyk, A. W.; Hackelöer, H. J.; Münter, R.; Tamler, H.; Kanert, O. *J. Phys., Colloq.* **1980**, *41*, C6-146.
(171) Tamler, H.; Kanert, O.; Alsem, W. H. M.; De Hossan, J. Th. M. *Acta Metall.* **1982**, *30*, 1523.
(172) Massiot, D.; Bessada, C.; Echegut, P.; Coutures, J. P. *Solid State Ionics* **1990**, *37*, 223.
(173) Junke, K. D.; Mali, M.; Roos, J.; Brinkman, D.; Lunden, A.; Graneli, B. *Solid State Ionics* **1988**, *28-30*, 1287.
(174) Topic, B.; Haeberlen, U.; Blinc, R. *Z. Phys. B - Condens. Matter* **1990**, *79*, 275.
(175) Amm, D. T.; Segel, S. L. In *XXIInd Congress Ampère*; Müller, K. A.; Kind, R.; Roos, J., Eds.; University of Zürich: Zürich, 1984; p 52.
(176) Jäger, C.; Heide, K. *J. Phys. C: Solid State Phys.* **1983**, *16*, L159.
(177) Spearing, D.; Farnan, I.; Stebbins, J. F. *EOS, Trans. Am. Geophys. Union* **1990**, *71*, 1671.
(178) Phillips, B. L.; Kirkpatrick, R. J.; Thompson, J. G. *EOS, Trans. Am. Geophys. Union* **1990**, *71*, 1671.
(179) Rigamonti, A. *Adv. Phys.* **1984**, *33*, 115.
(180) Rigamonti, A. In *Structural Phase Transitions, II*; Muller, K. A.; Thomas, H., Eds.; Springer-Verlag: Berlin, 1990; p 83.
(181) Bonera, G.; Borsa, F.; Rigamonti, A. *J. Phys., Colloq.* **1972**, *33*, C2-195.
(182) D'Ariano, G.; Aldrovandi, S.; Rigamonti, A. *Phys. Rev. B* **1982**, *25*, 7044.
(183) Volkov, S. V. *Pure Appl. Chem.* **1987**, *59*, 1151.
(184) Wilkes, J. S. In *Molten Salt Chemistry*; Mamantov, G.; Marassi, R., Eds.; Reidel: Amsterdam, 1987; p 217.
(185) Wilkes, J. S.; Frye, J. S.; Reynolds, G. F. *Inorg. Chem.* **1983**, *22*, 3870.
(186) Davis, L. P.; Dymek, C. J., Jr.; Stewart, J. P.; Clark, H. P.; Laudedale, W. J. *J. Am. Chem. Soc.* **1985**, *107*, 5041.
(187) Matsuo, T.; Ohno, H. *J. Chem. Phys.* **1985**, *82*, 3968.
(188) Nakamura, Y.; Kitazawa, Y.; Shimoji, M.; Shimokawa, S. *J. Phys. Chem.* **1983**, *87*, 5117.
(189) Hafner, S.; Nachtreib, N. H. *J. Chem. Phys.* **1965**, *42*, 631.
(190) Hafner, S.; Nachtreib, N. H. *J. Chem. Phys.* **1964**, *40*, 2891.
(191) Janes, N.; Oldfield, E. *J. Am. Chem. Soc.* **1985**, *107*, 6769.
(192) Englehard, G.; Michel, D. *High-Resolution Solid-State NMR of Silicates and Zeolites*; Wiley: New York, 1987.
(193) Stebbins, J. F.; Kanzaki, M. *Science* **1991**, *251*, 294.
(194) Ngai, L. H. *J. Phys. Chem. Solids* **1969**, *30*, 571.
(195) Nakamura, Y.; Baba, K.; Shimoji, M.; Shimokawa, S. *Ber. Bunsenges. Phys. Chem.* **1984**, *88*, 398.
(196) Nakamura, Y.; Shimokawa, S. *Ber. Bunsenges. Phys. Chem.* **1985**, *89*, 371.
(197) Funaki, J.; Nakamura, Y.; Shimokawa, S. *High Temp. Mater. Proc.* **1989**, *8*, 225.
(198) Nakamura, Y.; Funaki, J.; Shimokawa, S. In *Proceedings of the Joint International Symposium on Molten Salts*; Mamantov, G.; Hussey, C.; Saboungi, M.; Blander, M.; Mamantov, C.; Wilkes, J., Eds.; Electrochemical Society: Pennington, NJ, 1987; p 424.
(199) Margheritis, C. *Z. Naturforsch.* **1984**, *39a*, 1112.
(200) Harold-Smith, D. *J. Chem. Phys.* **1974**, *60*, 1405.
(201) Filho, W. W.; Havill, R. L.; Titman, J. M. *J. Magn. Reson.* **1982**, *49*, 296.
(202) Filho, W. W.; Havill, R. L.; Titman, J. M. *J. Phys. C: Solid State Phys.* **1982**, *15*, 3617.
(203) Sotier, S.; Jäger, W. *Z. Phys. Chem., Neue Folge* **1988**, *156*, 203.
(204) Sotier, S.; Warren, W. W., Jr. *J. Phys., Colloq.* **1980**, *41*, C8-40.
(205) Warren, W. W., Jr.; Sotier, S.; Brennert, G. F. *Phys. Rev. Lett.* **1983**, *50*, 1505.
(206) Warren, W. W., Jr.; Sotier, S.; Brennert, G. F. *Phys. Rev. B* **1984**, *30*, 65.
(207) Dupree, R.; Rogers, A. T. *Z. Phys. Chem., Neue Folge* **1988**, *156*, 177.
(208) Dupree, R.; Gardner, J. A. *J. Phys., Colloq.* **1980**, *41*, C8-20.
(209) Dupree, R.; Warren, W. W., Jr. In *Liquid Metals 1976*; Evans, R.; Greenwood, D. A., Eds.; Institute of Physics: London, 1977; p 454.
(210) Knight, W. D.; Berger, A. G. *Ann. Phys.* **1959**, *528*, 173.
(211) Zamir, D.; El-Hanany, U. *Pure Appl. Chem.* **1972**, *32*, 339.
(212) Seymour, E. F. W. *Pure Appl. Chem.* **1974**, *40*, 41.
(213) Winter, J. *Magnetic Resonance in Metals*; Oxford: Clarendon Press: Oxford, 1971.
(214) Shimoji, M.; Itami, T. *Atomic Transport in Liquid Metals*; Trans Tech Publications: Switzerland, 1986.
(215) Faber, T. E. *Introduction to the Theory of Liquid Metals*; Cambridge University Press: Cambridge, 1972.
(216) March, N. H. *Liquid Metals: Concepts and Theory*; Cambridge University Press: Cambridge, 1990.
(217) Warren, W. W., Jr. In *Charge Transfer/Electronic Structure of Alloys*; Bennett, L. H.; Willens, R. H., Eds.; Metallurgical Society: N.Y., 1974; p 223.
(218) Haas, H. *Z. Naturforsch.* **1986**, *41a*, 78.
(219) Ackermann, H.; Heitjans, P.; Stöckmann, H. J. Hyperfine Interactions of Radioactive Nuclei. Topics in Current Physics; Christiansen, J., Ed.; Springer-Verlag: Berlin, 1983; Vol. 31, p 291.
(220) Shaham, M.; El-Hanany, U.; Zamir, D. *Phys. Rev. B* **1978**, *17*, 3513.
(221) El-Hanany, U.; Zamir, D. *Phys. Rev. B* **1972**, *5*, 30.
(222) Kanert, O.; Küchler, R.; Recktenwald, J. *Solid State Commun.* **1980**, *33*, 993.
(223) El-Hanany, U.; Brennert, G. F.; Warren, W. W., Jr. *Phys. Rev. Lett.* **1983**, *50*, 540.
(224) Warren, W. W., Jr. In *Amorphous and Liquid Metals*; Lüscher, E.; Fritsch, G.; Jacucci, G., Eds.; Martinus Nijhoff: Dordrecht, 1987; p 304.
(225) Warren, W. W., Jr.; El-Hanany, U.; Brennert, G. F. *J. Non-Cryst. Solids* **1984**, *61 & 62*, 23.
(226) Warren, W. W., Jr.; Brennert, G. F.; El-Hanany, U. *Phys. Rev. B* **1989**, *39*, 4038.
(227) Dupree, R.; Kirby, D. J.; Gardner, J. A. In *Nuclear and Electron Resonance Spectroscopies Applied to Materials Science*; Kaufmann, E. N.; Shenoy, G. K., Eds.; Elsevier North Holland: Amsterdam, 1981; p 481.
(228) Hinkel, V.; Ploumbidis, D. *Z. Naturforsch.* **1984**, *39a*, 148.
(229) Hinkel, V.; Ploumbidis, D. *Phys. Stat. Sol. B* **1984**, *122*, K45.
(230) Ploumbidis, D.; Haghani, M. *Phys. Lett.* **1984**, *101A*, 52.
(231) Haghani, M. A.; Brinkmann, R.; Von Hartrott, M.; Maxim, P.; Ott, K.; Paulick, C. A.; Quitmann, D. In *Amorphous and Liquid Metals*; Lüscher, E.; Fritsch, G.; Jacucci, G., Eds.; Martinus Nijhoff: Dordrecht, 1987; p 405.
(232) Van der Marel, C.; Geertsma, W.; Van der Lugt, W. *J. Phys. F. Met. Phys.* **1980**, *10*, 2305.
(233) Meijer, J. A.; Kuiper, C.; Van der Marel, C.; Van der Lugt, J. *Z. Phys. Chem., Neue Folge* **1988**, *156*, 623.
(234) Ploumbidis, D.; Böss, E. *Phys. Stat. Sol. B* **1981**, *107*, 225.

(235) Dupree, R.; Rogers, A. T.; Freyland, W. *Philos. Mag. B* **1986**, *53*, 247.
(236) Dupree, R.; Kirby, D. J.; Freyland, W. *Philos. Mag. B* **1982**, *46*, 595.
(237) Dupree, R.; Bottyan, L.; Freyland, W.; Rogers, A. T. *J. Non-Cryst. Solids* **1984**, *61 & 62*, 53.
(238) Dupree, R.; Kirby, D. J.; Freyland, W.; Warren, W. W., Jr. *Phys. Rev. Lett.* **1980**, *45*, 130.
(239) Dupree, R.; Kirby, D. J.; Freyland, W.; Warren, W. W., Jr. *J. Phys., Colloq.* **1980**, *41*, C8–16.
(240) Ott, K.; Dürrwächter, M.; Hagnani, M. A.; Von Hartrott, M.; Sauer, B.; Quitmann, D. *J. Non-Cryst. Solids* **1989**, *114*, 828.
(241) Ott, K.; Dürrwächter, M.; Haghani, M. A.; Sauer, B.; Quitmann, D. *Europhys. Lett.* **1989**, *10*, 759.
(242) Senel, I.; Ploumbidis, D.; Quitmann, D. *J. Phys. Condens. Matter* **1989**, *1*, 4223.
(243) Rünger, R.; Ploumbidis, D. *Phys. Status Solidi B* **1984**, *122*, K 49.
(244) Ploumbidis, D.; Hüber, G. *Z. Naturforsch.* **1982**, *37a*, 319.
(245) Ploumbidis, D.; Rünger, R.; Bucklisch, R. *Z. Naturforsch.* **1981**, *36a*, 1305.
(246) Rünger, R.; Ploumbidis, D. *Z. Naturforsch.* **1984**, *39a*, 145.
(247) Clark, W. G.; Wong, W. H.; Hines, W. A.; Lan, M. D.; MacLaughlin, D. E.; Fisk, Z.; Smith, J. L.; Ott, H. R. *J. Appl. Phys.* **1988**, *63*, 3890.
(248) Chabre, Y.; Segransan, P.; Berthier, C.; Di Salvo, F. J.; Fischer, J. E. *Synth. Met.* **1983**, *8*, 7.
(249) Borsa, F.; Corti, M.; Rigamonti, A.; Torre, S. *Phys. Rev. Lett.* **1984**, *53*, 2101.
(250) Holcomb, D. F.; Norberg, R. E. *Phys. Rev.* **1955**, *98*, 1074.
(251) Seymour, E. F. W. *Proc. Phys. Soc.* **1953**, *A66*, 85.
(252) Stoebe, T. G.; Gulliver, R. D., II; Ogurtani, T. O.; Huggins, R. A. *Acta Metall.* **1965**, *13*, 701.
(253) Hanabusa, M.; Bloembergen, N. *J. Phys. Chem. Sol.* **1966**, *27*, 363.
(254) Murday, J. S.; Cotts, R. M. *J. Chem. Phys.* **1968**, *48*, 4938.
(255) Murday, J. S.; Cotts, R. M. *Z. Naturforsch.* **1971**, *26a*, 85.
(256) Krüger, G. J.; Müller-Warmuth, W.; Klemm, A. *Z. Naturforsch.* **1971**, *26a*, 94.
(257) Bucklisch, R.; Ploumbidis, D. *Z. Naturforsch.* **1981**, *36a*, 1155.
(258) Marsden, J.; Havill, R. L.; Titman, J. M. *J. Phys. F. Met. Phys.* **1980**, *10*, 1589.
(259) Havill, R. L.; Marsden, J.; Titman, J. M. *J. Phys. F: Met. Phys.* **1977**, *7*, 2357.
(260) Bosse, J.; Quitmann, D.; Wetzel, C. *Phys. Rev. A* **1983**, *28*, 2459.
(261) Brinkmann, R.; Elwenspoek, M.; Maxim, P.; Quitmann, D. *Hyperfine Interactions* **1983**, *15/16*, 581.
(262) Maxim, P.; Brinkmann, R.; Paulick, C. A.; Elwenspoek, M.; Von Hartrott, M.; Kiehl, M.; Quitmann, D. *Z. Naturforsch.* **1986**, *41a*, 118.
(263) Willeke, F.; Von Hartrott, M.; Quitmann, D. *J. Phys. F: Met. Phys.* **1981**, *11*, 275.
(264) Rossbach, J.; Von Hartrott, M.; Höhne, J.; Quitmann, D.; Weihreter, E.; Willeke, F. *J. Phys. F: Met. Phys.* **1980**, *10*, 729.
(265) Ott, K.; Hagnani, M. A.; Paulick, C. A.; Quitmann, D. *Prog. NMR Spectrosc.* **1989**, *21*, 203.
(266) Ott, K.; Hagnani, M. A.; Kiehl, M.; Paulick, C. A.; Quitmann, D. *Z. Phys. Chem., Neue Folge* **1988**, *156*, 635.
(267) Ott, K.; Kiehl, M.; Hagnani, M.; Von Hartrott, M.; Maxim, P.; Paulick, C. A.; Quitmann, D. In *Amorphous and Liquid Metals*; Lüscher, E.; Fritsch, G.; Jacucci, G., Eds.; Martinus Nijhoff: Dordrecht, 1987; p 312.
(268) Quitmann, D. In *Amorphous and Liquid Metals*; Lüscher, E.; Fritsch, G.; Jacucci, G., Eds.; Martinus Nijhoff: Dordrecht, 1987; p 279.
(269) Elwenspoek, M.; Maxim, P.; Brinkmann, R.; Weihreter, E.; Quitmann, D. *Phys. Lett.* **1983**, *96A*, 435.
(270) Elwenspoek, M.; Brinkmann, R.; Maxim, P.; Paulick, C.; Quitmann, D. *Ber. Bunsenges. Phys. Chem.* **1983**, *87*, 823.
(271) Elwenspoek, M.; Brinkmann, R.; Von Hartrott, M.; Kiehl, M.; Maxim, P.; Paulick, C. A.; Quitmann, D. *Hyperfine Interactions* **1983**, *15/16*, 577.
(272) Maxim, P.; Brinkmann, R.; Elwenspoek, M.; Von Hartrott, M.; Kiehl, M.; Paulick, C. A.; Quitmann, D. *Hyperfine Interactions* **1983**, *15/16*, 573.
(273) Von Hartrott, M.; Höhne, J.; Quitmann, D.; Rossbach, J.; Weihreter, E.; Willeke, F. *Phys. Rev. B* **1979**, *19*, 3449.
(274) Van der Marel, C.; Heitjans, P.; Ackermann, H.; Ackermann, H.; Bader, B.; Freiländer, P.; Schirmer, A.; Stöckmann, H. J. *Z. Phys. Chem., Neue Folge* **1988**, *156*, 629.
(275) Heitjans, P.; Kiese, G.; Van der Marel, C.; Ackermann, H.; Bader, B.; Freiländer, P.; Stöckmann, H. J. *Hyperfine Interactions* **1983**, *15/16*, 569.
(276) Kruglov, V. F.; Verkhovskiy, S. V.; Kleshchev, G. V. *Fiz. Met. Metalloved.* **1983**, *55*, 617.
(277) Bottyan, L.; Berke, D. L.; Tompa, K. *Phys. Status Solidi B* **1983**, *118*, 835.
(278) Shaham, M. *Phys. Rev. B* **1979**, *20*, 878.
(279) Chabre, Y.; Segransan, P. *Solid State Commun.* **1975**, *17*, 1529.
(280) Tiers, J. F.; Chabre, Y. *J. Phys. F: Met. Phys.* **1981**, *11*, 1943.
(281) Carlos, W. E.; Taylor, P. C. *J. Phys. Colloq.* **1981**, *42*, C4–725.
(282) Barnes, R. G.; Jerosch-Herold, M.; Shinar, J.; Borsa, F.; Torgeson, D. R.; Peterson, D. T.; Lucas, A. J.; Styles, G. A.; Seymour, E. F. W. *Phys. Rev. B* **1987**, *35*, 890.
(283) Barnes, R. G.; Borsa, F.; Jerosch-Herold, M.; Han, J. W.; Belhoul, M.; Shinar, J.; Torgeson, D. R.; Peterson, D. T.; Styles, G. A.; Seymour, E. F. W. *J. Less-Common Metals* **1987**, *129*, 279.
(284) Richards, P. M. *Phys. Rev. B* **1987**, *36*, 7417.
(285) Han, J. W.; Lichty, L. R.; Torgeson, D. R.; Seymour, E. F. W.; Barnes, R. G.; Billeter, J. L.; Cotts, R. M. *Phys. Rev. B* **1989**, *40*, 9025.
(286) Barnfather, K. J.; Seymour, E. F. W.; Styles, G. A.; Dianoux, A. J.; Barnes, R. G.; Torgeson, D. R. *Z. Phys. Chem., Neue Folge* **1989**, *164*, 935.
(287) Barnes, R. G. *Z. Phys. Chem., Neue Folge* **1989**, *164*, 841.
(288) Bustard, L. D.; Cotts, R. M.; Seymour, E. F. W. *Phys. Rev. B* **1980**, *22*, 12.
(289) Zogal, O. J.; Cotts, R. M. *Phys. Rev. B* **1975**, *11*, 2443.